Structure-Function Relationships in L-Amino Acid Deaminase, a Flavoprotein Belonging to a Novel Class of Biotechnologically Relevant Enzymes

Paolo Motta[‡,1], Gianluca Molla[‡,§,1,2], Loredano Pollegioni[‡,§], Marco Nardini[†,3]

From the [‡]Dipartimento di Biotecnologie e Scienze della Vita, Università degli Studi deII'Insubria, via J. H. Dunant 3, 21100 Varese, Italy, [§]The Protein Factory, Politecnico di Milano and Università degli Studi deII'Insubria, Varese, Italy
[†]Dipartimento di Bioscienze, Università degli Studi di Milano, via Celoria 26, Italy 20133 Milano, Italy

Running title: *Structure-function relationships in L-amino acid deaminase*

[1]These authors contributed equally to this work.
[2]To whom the correspondence should be addressed: Prof. G. Molla, Dipartimento di Biotecnologie e Scienze della Vita, Università degli Studi deII'Insubria, via J. H. Dunant 3, 21100 Varese, Italy, Telephone: ++39 0332 421414; FAX: ++39 0332 421500; E-mail: gianluca.molla@uninsubria.it.
[3]To whom the correspondence should be addressed: Prof. M. Nardini, Dipartimento di Bioscienze, Università degli Studi di Milano, 20133 Milano, Italy, Telephone: ++39 02 50314898; FAX: ++39 02 50314895; E-mail: marco.nardini@unimi.it

Keywords: L-amino acid deaminase, flavoprotein, membrane-bound enzyme, enzyme structure, structure-function, conformational change, protein engineering, X-ray crystallography

ABSTRACT

L-Amino acid deaminase from *Proteus myxofaciens* (PmaLAAD) is a membrane flavoenzyme which catalyses the deamination of neutral and aromatic L-amino acids into α-keto acids and ammonia. PmaLAAD does not use dioxygen to reoxidize reduced $FADH_2$ and thus does not produce hydrogen peroxide; instead, it uses cytochrome b-like protein as electron acceptor. Although the overall fold of this enzyme resembles the one of known amine or amino acid oxidases, it shows specific structural features: an additional, novel α+β subdomain (likely involved in recruiting the electron-acceptor partner), a solvent exposed FAD isoalloxazine ring, a large and open active site. In addition, PmaLAAD requires substrate-induced conformational changes of part of the active site, in particular Arg316 and Phe318, to reach the correct geometry for catalysis. These studies are expected to pave the way to the rational improvement of the versatility of this flavoenzyme, which is critical for the field of biocatalysis of enantiomerically pure amino acids.

A variety of enzymes has been used to prepare chiral pharmaceutical and agricultural compounds containing enantiomeric amine or amino acid groups. Among these, aminotransferases (AT, EC 2.6.4.X), lipases (EC 3.1.1.X), amine oxidases (EC 1.4.3.22), amino acid dehydrogenases (EC 1.4.1.X) and amino acid oxidases (EC 1.4.3.X) (1,2).

The deracemization of a racemic amino acid to obtain the L- configuration has been achieved by using a stereoselective D-amino acid oxidase (DAAO, EC 1.4.3.3) followed by a chemical reduction. The second step iteratively converts the imino acid produced (from the D-amino acid) back into a D,L-mixture to obtain the full resolution of the racemic mixture into the L-enantiomer (1). This approach needs stable recombinant DAAOs, possessing wide substrate specificity, as well as variants engineered to act on unnatural amino acids (3).

Amino acid oxidases with reverse stereoselectivity are also well known flavooxidases, mainly produced by snakes or by microorganisms. In particular, L-amino acid oxidases (LAAO, EC 1.4.3.2) catalyse the stereoselective oxidative deamination of L-amino acids into the corresponding α-keto acids and ammonia: the reoxidation of $FADH_2$ by dioxygen then generates H_2O_2 (4). These flavoenzymes catalyse an irreversible reaction (differently from AT) and do not need a specific step of cofactor regeneration, as instead required by the NAD-dependent dehydrogenases. Because of the problematic overexpression of snake venom LAAOs in recombinant hosts and the limited substrate acceptance of the microbial

counterparts, no appropriate LAAOs for biocatalysis are available (4).

L-amino acid deaminases (LAADs) represent a suitable alternative to LAAOs. LAAD (first identified in the genera *Proteus*, *Providencia* and *Morganella*) catalyses the deamination of L-isomer of amino acids yielding the corresponding α-keto acids and ammonia without any evidence of H_2O_2 production. LAAD from *Proteus myxofaciens* (PmaLAAD), expressed in *E. coli* K12 strain, shows a preference for L-amino acids containing aliphatic, aromatic and sulphur containing side chains (5). Notwithstanding the reaction catalysed by LAAD is of both scientific and practical interest (5-7), although no details about its structural-functional relationships and biological significance have been reported so far.

In order to gain more insight into the properties of LAAD, we expressed the *P. myxofaciens* enzyme in *E. coli* and demonstrated that it is a membrane flavoenzyme employing a cytochrome b-like protein as electron acceptor. Protein engineering studies allowed producing a truncated, soluble form, which was crystallized. Its structural and biochemical characterization clearly shows that LAAD does not belong to the LAAO subfamily of flavooxidases and it is characterized by a large and open active site. These studies will provide the strong background needed for the rational alteration of the versatility of this flavoenzyme, which is critical to push novel applications in biocatalysis.

EXPERIMENTAL PROCEDURES

Cloning of Wild-type Variants of PmaLAAD—The gene encoding for LAAD from *Proteus myxofaciens* (newly classified as *Cosenzaea myxofaciens*) (8) cloned into the *NdeI* and *SalI* restriction sites of the pET21a expression plasmid (Merck) was a generous gift of Wolfgang Kroutil (University of Graz).

PmaLAAD-00N, -01N, -02N and -00C variants (Fig. 1) were produced by PCR. PmaLAAD wild-type gene was amplified using the upstream primers Var00-UP (5'-TAGGCTAGCAACATTTCAAGGAGAAAGC TAC-3'), Var01-UP (5'-TAGGCTAGCATGGTTCGCCGTGATGGTAA A-3') or VAR02-UP (5'-ATTGCTAGCGCCCTGCCATCAGAATCTGA TG-3') or VAR00C-UP (5'-TAGCATATGAACATTTCAAGGAGAAAGC TAC-3'); as downstream primer, the primer Var00-DN (5'-GCACGGATCCTTATTACTTCTTAAAACGA TCCAAACTAAACGG-3') was used for the -00N, -01N and -02N mutants and VAR00C-DN (5'-CGCACCTCGAGCTTCTTAAAACGATCCAA AC-3') for the -00C mutant. The primers were designed to insert a *NheI* restriction site at the 5'-end and a *BamHI* restriction site at the 3'-end of the amplification products. The amplification products (Pma-VAR00, -VAR01 and -VAR02 genes) were subcloned into the *Nhe*I and *BamHI* restriction sites of pET11a-His vector (a modified pET11a vector encoding a 6xHisTag sequence which is added at the N-terminus of the recombinant protein) (9) generating the pET11a-His-PMA00, pET11a-His-PMA01 and pET11a-His-PMA02 plasmids. Similarly, the pET24b plasmid was used to generate the pET24b-Pma00C-His expression plasmid by using the *NdeI* and *XhoI* restriction sites. The expressed proteins possess a HisTag sequence (Fig. 1). The sequences of the cloned genes were confirmed by gene sequencing.

Screening of Expression Conditions for PmaLAAD Wild-type and Variants—Expression conditions for PmaLAAD and its variants were screened by a simplified 96-well microplate factorial design approach (10). Four different *E. coli* strains (*E. coli* BL21(DE3), BL21(DE3)pLysS, Origami2(DE3) and Rosetta2(DE3)pLysS strains - Novagen) and two media (LB or modified TB, added with 10 g/L glycerol) were used. After overnight incubation at 28 °C, protein expression was induced by adding 0.005 or 0.1 mM final concentration of IPTG. Cells were collected after 4 h (at 28 °C) or 20 h (at 15 °C). PmaLAAD expression was assessed by activity assay on cell lysates by the spectrophometric assay (see below), as well as by Western blot analysis using anti-HisTag antibodies (Santa Cruz).

Expression and Purification of Wild-type and Variants of PmaLAAD—Recombinant wild-type PmaLAAD was expressed in *E. coli* BL21(DE3) strain in the following conditions: cells (from a single colony) were grown in modified TB medium (containing 10 g/L glycerol) added with 100 μg/mL ampicillin. Protein expression was induced by adding 0.1 mM IPTG at an OD_{600nm} = 0.5; after 4 hours of growth at 28 °C cells were harvested by centrifugation.

E. coli recombinant cells expressing

PmaLAAD were lysed by sonication in lysis buffer (50 mM potassium phosphate pH 7.0, 5 mM $MgCl_2$). The cell lysate was separated from the cell debris by centrifugation at 38,500 g for 1 h yielding the insoluble fraction of the cell lysate and the crude extract containing the soluble proteins and small membrane fragments. Ultracentrifugation of the latter fraction at 150,000 g for 2 h produced a membrane fraction (pellet) and a cytoplasmic fraction (supernatant). See Fig. 2 for details.

The purification of recombinant PmaLAAD-00N, -00C, and -01N was carried out by metal-affinity chromatography on a HiTrap Chelating column: PmaLAAD variants were eluted at 500 mM imidazole.

Activity Assay—The specific activity on L-Phe was assayed spectrophotometrically at 321 nm by following the formation of the product phenylpyruvate (5). The protein sample was added to 2 mL (final volume) of 25 mM L-Phe in 50 mM potassium phosphate buffer, pH 7.5, and incubated for 2 min at 25 °C. Every 30 s an aliquot of 400 µL was transferred into a plastic cuvette containing 400 µL of 3 N NaOH to stop the reaction and allow colour development. One enzymatic unit corresponds to the amount of enzyme that converts 1 µmol of L-Phe per minute. Alternatively, an oxygen consumption assay was used to investigate the effect of different membrane preparations on LAAD activity (11).

Apparent K_m and V_{max} values for L-Phe were determined by the phenylpyruvate production assay using increasing substrate concentrations, at 25 °C and oxygen air saturation (0.253 mM).

pH and Temperature Optimum Determination—For the investigation of the pH dependence of the initial rate of phenylpyruvate production, wild-type PmaLAAD enzymatic activity was assayed at different pH values on 25 mM L-Phe in a multicomponent buffer (160 mM Tris–HCl, 160 mM Na_2CO_3, 160 mM H_3PO_4, 650 mM KCl and 1% glycerol), at room temperature (12).

Temperature dependence of PmaLAAD activity was assayed by measuring the production of phenylpyruvate as described above at different temperatures, in 50 mM potassium phosphate, pH 7.5, using 25 mM L-Phe as substrate.

Spectral Measurements—Absorbance spectra in the UV–visible region, as well as ligand binding experiments, were recorded using a Jasco V-560 spectrophotometer as previously reported (13).

Anaerobic samples were prepared in anaerobic cuvettes by applying ten cycles of evacuation and then flushing with oxygen-free argon. Flavin reduction was carried out by adding ≈ 15 µM, 30 µM or 25 mM (final concentrations) of the substrate L-Phe to samples containing ≈ 15 µM enzyme; reduction of the cofactor for PmaLAAD-00N variant was performed both in the absence and in the presence of *E. coli* membranes.

Photoreduction experiments were carried out at 4 °C using an anaerobic cuvette containing 18.5 µM PmaLAAD-00N or 13.1 µM PmaLAAD-01N, 5 mM EDTA and 0.5 µM 5-deaza FAD. The solution was photoreduced using a 250 W lamp and the progress of the reaction was monitored spectrophotometrically (13,14). At the end of the reaction, FAD cofactor was reoxidized anaerobically by adding 5.5 µM (final concentration) benzyl viologen. Photoreduction experiments for PmaLAAD-00 and -01N were performed both in the absence and in the presence of *E. coli* membranes.

Binding experiments of benzoate, anthranilate and sulfite to PmaLAAD-00N and -01N variants were performed by adding small volumes (5 – 50 µL) of concentrated stock solutions (0.1 mM – 1 M) to samples containing 0.8 mL of ≈ 15 µM enzyme (13,14).
All spectral measurements were recorded at 15 °C in 50 mM potassium phosphate buffer, pH 7.5, except where stated otherwise.

Crystallization, Structure Determination and Refinement—Crystallization trials of PmaLAAD-01N (≈ 10 mg/mL) were performed using the sitting drop vapour diffusion method with an Oryx-8 crystallization robot (Douglas Instruments, East Garston, UK). After a week at 4 °C, crystals were observed under the following growth condition: 15% PEG 6K, 0.1 M MES (pH 6.5), 10% MPD. They were cryoprotected in the mother liquor (20% PEG 6K, 0.1 M MES, pH 6.5, 10% MPD) supplemented with 15% glycerol, and flash-frozen in liquid nitrogen. A single crystal, belonging to the monoclinic space group $P2_1$, diffracted up to 2.0 Å resolution. Diffraction data were collected at the ESRF beamline ID23-2 (Grenoble, France) and processed with XDS (15) and SCALA (16).

The PmaLAAD-01N structure was solved by molecular replacement using the program Phaser (17), with the β-subunit of sarcosine oxidase from *Pseudomonas maltophilia* (PDB code 2GAG)

(18) as a search model. Two protein molecules were located in the crystal asymmetric unit and were subjected to rigid-body and restrained refinement using Phenix (19). The amino acid sequence of the model was modified to match the correct sequence and manually fitted to the electron density using the program Coot (20). A set of restrained refinement cycles were performed using the programs Phenix (19) and Refmac (21). The final refined PmaLAAD-01N structure (R_{factor} = 16.6%, R_{free} = 21.1%) contains 2x447 protein residues (28-474), 2 FAD cofactors, and 521 water molecules, with good stereochemical parameters.

For soaking experiments and data collection, native PmaLAAD-01N crystals were removed from the crystallization drop with a nylon loop and soaked overnight in a mixture of their mother liquor supplemented with 20 mM anthranilate. The soaked crystals were quickly pulled through a drop of cryoprotectant before being flash-cooled in liquid nitrogen. A single crystal, belonging to monoclinic space group $P2_1$, diffracted up to 1.75 Å resolution (data collection and processing as above).

The structure of the PmaLAAD-01N/anthranilate complex was determined by molecular replacement using the program Phaser (17), with the structure of PmaLAAD-01N as a search model. Two protein molecules were located in the crystal asymmetric unit. The structure was then remodelled with Coot (20) and restrained refined, with anisotropic B-factors, using the program Refmac (21). After a few cycles of refinement, the 2Fo-Fc electron density map showed structural details that allowed unambiguous modelling of the bound substrate-analogue. The final model (R_{factor} = 13.4%, R_{free} = 19.4%) contains 2x447 protein residues (28-474), 2 FAD cofactors, and 537 water molecules, with good stereochemical parameters.

All data reduction and refinement statistics for both protein models (PmaLAAD-01N and PmaLAAD-01N/anthranilate complex) are reported in details in Table 1. The stereochemical quality of the models was assessed with MolProbity (22).

The atomic coordinates and structure factors for PmaLAAD-01N and PmaLAAD-01N/anthranilate complex (codes 5FJM, 5FJN respectively) have been deposited in the Protein Data Bank (http://www.wwpdb.org/).

RESULTS

Purification of Recombinant Wild-type PmaLAAD—Recombinant PmaLAAD (which sequence is reported in Fig. 1*B*) was expressed in *E. coli* BL21(DE3) cells. After ultracentrifugation of the crude extract, the recombinant enzyme was largely found associated to the membrane fraction (*i.e.* in the pellet fraction). Detergents were not effective in solubilizing active PmaLAAD (not shown). Ultracentrifugation resulted into a partial purification of PmaLAAD (≈ 2-fold, Fig. 2). Interestingly, thawing, diluting (5-fold) and centrifuging the membrane fraction stored at -80 °C resulted in a phase separation: the lower, denser phase was enriched in PmaLAAD (≈ 40-50% of PmaLAAD based on the enzymatic activity and SDS-PAGE analysis) thus resulting into a further ≈ 2.5-fold increase in specific activity, reaching ≈ 2.9 U/mg of protein (Fig. 2).

By size exclusion chromatography, most of PmaLAAD from the membrane fraction eluted in a peak corresponding to a molecular mass > 600 kDa (*i.e.* associated to large membrane fragments containing additional proteins), while a small fraction eluted in a peak corresponding to ≈ 50 kDa (a value close to the expected theoretical mass of 51.5 kDa). PmaLAAD activity was associated to the previous fraction, this suggesting that PmaLAAD was active when associated to the cellular membranes. In addition, a N- and a C-terminal His-tagged full-length proteins were produced (PmaLAAD-00N and -00C, respectively, Fig. 1) and expressed at a level similar to that of PmaLAAD by using BL21(DE3) or Origami *E. coli* strains.

When the resuspended membrane fraction containing PmaLAAD-00N (specific activity on L-Phe of 0.55 U/mg protein) was loaded on an HiTrap chelating column it separated into two fractions: the flow-through one containing the active enzyme (≈ 100 U/L fermentation broth, 64% of purification yield) associated to membrane fragments, and the fraction eluted at 0.5 M imidazole which contained a significant part of PmaLAAD-00N (devoid of membranes). The LAAD activity of the latter fraction was marginal (5 U/L fermentation broth) and the purity degree was ≈ 70%, as estimated by SDS-PAGE analysis. A comparable result was obtained when the crude extract was directly loaded on the HiTrap column (*i.e.*, omitting the ultracentrifugation step). Similar results were obtained for the PmaLAAD-00C which possesses a slightly lower specific activity (0.45 vs 0.55 U/mg protein). Following HiTrap chelating

column, the enzymatic activity was detected in the flow-through fraction only (≈ 250 U/L fermentation broth) while the fraction eluted at 0.5 M imidazole contained a significant part of PmaLAAD-00C and possessed only a marginal LAAD activity (< 2%, with a purity ≈ 70%, as estimated by SDS-PAGE analysis).

Notably, PmaLAAD in the crude extract showed a fairly good stability since it retained its enzymatic activity up to 6 hours and showed a 50% decrease only after 24 hours of incubation at 25 °C. The enzyme retained ≈ 50% and ≈ 75% of the original activity when stored for 1 month in the presence of 10% glycerol at -20 °C and at -80 °C (even without glycerol), respectively.

Biochemical Properties of Recombinant PmaLAAD—The specific activity of PmaLAAD in the crude extract (≈ 0.6 U/mg protein) on 25 mM L-Phe as substrate was identical when assayed as production of phenylpyruvic acid or as O_2 consumption (*i.e.* by polarographic assay) (11). However, the latter assay was feasible only for PmaLAAD in the membrane fraction (see below). The dependence of the initial rate *vs.* L-Phe concentration and at 0.253 mM oxygen is shown in Fig. 3*A*: the $K_{m,app} = 3.27 \pm 0.96$ mM and $V_{max,app} = 1.35 \pm 0.08$ U/mg protein are in good agreement with the values reported in literature ($K_{m,app}$ = 2.3 mM, $V_{max,app}$ = 2 U/mg) (5). No substrate inhibition was evident up to 100 mM L-Phe.

Noteworthy, no halving of oxygen consumption was observed by adding a large excess of catalase to the reaction mixture of the polarographic assay, this demonstrating that no H_2O_2 was produced during the reaction. Lack of H_2O_2 production was also confirmed by the classic *o*-dianisidine/peroxidase spectrophotometric coupled assay used for flavoprotein oxidases (11). Similarly, no superoxide was produced by PmaLAAD reaction since the O_2-consumption was not modified by adding 1.6-24 U of superoxide dismutase. Indeed, O_2-concentration did not affect the activity of PmaLAAD: a similar apparent activity was determined at ≥ 10% O_2-saturation.

The relative substrate specificity of PmaLAAD toward natural and unnatural amino acids was determined by the polarographic method using a fixed volume of membrane-associated PmaLAAD (corresponding to ≈ 0.5 mg of total membrane proteins) and 25 mM substrate concentration. As shown in Table 2, PmaLAAD is specific for aromatic, neutral L-amino acids; a low activity was assayed towards small, charged or polar L-amino acids. Notably, a significant activity (33% in comparison to L-Phe) was also measured on the unnatural amino acid L-phenylalanine ethylester, whose α-carboxylic group is esterified. No significant activity was assayed with D-amino acids (Table 2).

The pH dependence of PmaLAAD activity was evaluated on the sample from the membrane fraction by using the spectrophotometric assay in the 3 to 10 pH range (12). The highest activity is apparent at neutral pH (between 7 and 7.5) and is negligible below pH 5 and above pH 9 (Fig. 3*B*). Concerning the temperature dependence, the activity of PmaLAAD linearly increased up to 50 °C and then rapidly decreased becoming negligible at 70 °C (Fig. 3*C*). This behaviour resembles the one reported for LAAD from *P. mirabilis* (optimal temperature of 45 °C) (23).

On the Biological Activity of PmaLAAD: Effect of Membranes—Enzymatic activity assayed by the O_2-consumption method of the quasi-inactive fraction of purified PmaLAAD-00N (eluted from HiTrap column at 0.5 M imidazole, see above) was restored by adding an equal volume of membranes from *E. coli* BL21(DE3) cells (a microorganism not encoding for a LAAD) transformed with the pET11a mock plasmid. A 4.5-fold increase of activity was observed, that became ≈ 16-fold after sonication. Indeed, sonication of PmaLAAD-00N in the absence of membranes resulted into a 6-fold decrease of the original, low enzymatic activity. Similarly to PmaLAAD-00N, a ≈ 32-fold increase in enzymatic activity was apparent by adding *E. coli* membranes, prepared from 2.25 mg cells, to 75 μg of purified PmaLAAD-00C.

The effect of the amount of *E. coli* membranes on the activity of quasi-inactive PmaLAAD-00N (150 μg of protein) was also investigated. A huge increase in activity (≈ 12-fold) was obtained following the addition of an amount of membranes corresponding to ≈ 0.15 mg of cells for each μg of PmaLAAD-00N. Doubling the amount of added membranes resulted into the maximum observed increase in enzyme activity (≈ 50-fold): no further increase was obtained using larger amounts of membranes. Notably, no recovery of the enzymatic activity was observed using membranes from the microorganism *Streptomyces venezuelae* while only a low, partial recovery was apparent (2.7-fold) in the presence of membranes from the human glioblastoma T98G cells.

The dependence of PmaLAAD-00N activity

on a putative molecular partner associated to the bacterial membrane was also investigated by mixing the purified enzyme variant with two commercially available *E. coli* lipid extracts (Avanti Polar Lipids). Mixing 150 μg of PmaLAAD-00N with 4.5 mg of Total Lipid extract (containing 17.6% unknown components, mainly lipoproteins) resulted into a slight (4-fold) increase of activity, significantly lower as compared with the activity recovery observed using the same amount of *E. coli* membranes (= 32-fold). Employing the Polar Lipid extract (with a high degree of purity) only a 1.6-fold increase of enzymatic activity was apparent (Table 3). As a positive control, 150 μg of PmaLAAD-00N were mixed with 2.25 mg of lipid extract and a corresponding amount of *E. coli* membranes (22.5 mg): the recovery of the enzymatic activity resembled the value observed for *E. coli* membranes only.

Altogether, these results point to the need of specific membrane partner(s) for PmaLAAD enzymatic activity recovery, rather than an aspecific hydrophobic environment provided by bacterial membranes.

Spectral Characterization of PmaLAAD-00N—The spectral properties of the enzyme were assessed using the membrane-devoid PmaLAAD-00N variant because of its higher purity compared to the form lacking the HisTag and the absence of membranes. PmaLAAD-00N shows the canonical absorbance spectrum of FAD-containing flavoproteins with three main peaks at 277, 380 and 456 nm (Fig. 4*A*). The ratio between the absorbance at 277 nm and at 456 nm is quite high (≈ 17), and the estimated molar extinction coefficient is 14168 $M^{-1}cm^{-1}$ at 456 nm. Indeed, the absorbance spectrum of PmaLAAD-00C resembled the one of PmaLAAD-00N (data not shown): this indicates that the location of the HisTag does not affect the flavin environment of PmaLAAD. The far-UV circular dichroism spectrum shows that the recombinant PmaLAAD-00N is folded and contains secondary structure elements (not shown).

Amino acid oxidases are known to interact with a number of carboxylic acids yielding specific spectral modifications and thus representing useful active site probes (4,24,25). The binding of various putative ligands to PmaLAAD-00N was investigated in the absence and in the presence of *E. coli* membranes (corresponding to ≈ 0.15 mg of cells for each μg of PmaLAAD-00N). No spectral perturbations were evident up to ≈ 0.4 M sodium benzoate pointing to the inability of PmaLAAD-00N to bind this well-known DAAO ligand (24,26). However, when the same experiment was performed using anthranilate (2-aminobenzoate), specific spectral perturbations were observed in the 400-500 nm and in the 520-600 nm range (Fig. 4*C*); the latter spectral change resembles the charge transfer complex between the ligand and the FAD cofactor observed for other amino acid oxidases (24,26). These absorbance changes were more evident in the absence of membranes: from the absorbance changes at 533 nm as a function of anthranilate concentration, a K_d of 18.4 ± 4.4 mM was calculated (Fig. 4*C*, inset). The same experiment was performed using kojic acid as ligand (Fig. 4*E*), yielding a general increase in absorbance with a saturation behaviour in the visible region of the spectrum: K_d = 3.0 ± 0.3 mM (Fig. 4*E*, inset).

No spectral perturbations resembling flavin reduction were observed adding sulfite to PmaLAAD-00N (up to ≈ 0.45 M Na_2SO_3), this suggesting divergences in FAD reactivity between PmaLAAD and the enzymes belonging to the oxidase class of flavoproteins (27).

The PmaLAAD-00N variant was mixed under anaerobic conditions with an excess of substrate (25 mM L-Phe) both in the absence and in the presence of *E. coli* membranes. Under both circumstances, the FAD cofactor rapidly reacts with the substrate yielding the typical absorbance spectrum of the reduced FAD (*i.e.*, bleaching of the 450 nm peak in the dead time of mixing for the membrane-free preparation) (Fig. 4*A*). In the presence of membranes, FAD reduction was biphasic: the large, rapid decrease at 450 nm was followed by a slower and smaller further decrease (taking ≈ 15 min to completion, Fig. 4*B*). Interestingly, in the latter case three narrow absorbance peaks are evident following FAD reduction: one major peak at 429 nm and two minor peaks at 532 nm and 560 nm (Fig. 4*B*). These peaks correspond to the ones of the reduced form of cytochrome b (28), a small membrane protein usually associated to redox enzymes (29). When the same experiment was performed with stoichiometric amounts of L-Phe (1:1 or 1:2 enzyme:L-Phe ratios) in the absence of membranes, a partial and slow reduction of the flavin was observed (3.5 or 3.0 hours, respectively).

Noteworthy, a slow reduction of membrane-associated cytochrome b (requiring more than 1 hour to completion, data not shown) was observed also in the absence of exogenous PmaLAAD-00N. This suggests the presence in *E. coli*

membranes of a biochemical system(s) able to oxidise L-Phe and to transfer electrons to cytochrome b, even if at a much lower rate in comparison to PmaLAAD-00N. Actually, small amounts of free L-amino acids are present in *E. coli* membrane preparations since PmaLAAD-00N was slowly reduced under anaerobic conditions following membrane addition, a phenomenon not observed when the traces of L-amino acids were enzymatically removed.

Anaerobic photoreduction of PmaLAAD-00N in the presence of 5 mM EDTA and 0.5 μM 5-deaza-FAD was investigated both in the absence and in the presence of *E. coli* membranes (1:1 v/v ratio). The FAD cofactor of the free enzyme was reduced after 5 min of exposition to intense light radiation (Fig. 4*G*): the presence of membranes increased the rate of flavin reduction (3.5 min to reach complete reduction) (Fig. 4*H*). The spectra recorded during photoreduction in the absence of membranes showed two isosbestic points at 510 and 410 nm; the latter point was not conserved in the presence of membranes due to the presence of an additional spectral species, *i.e.* cytochrome b. A large amount of anionic semiquinone flavin form was evident both in the presence and in the absence of membranes, as made apparent by the large increase of a peak at ≈ 380 nm, an effect due to intense light irradiation. Notably, when the cuvette containing fully photoreduced PmaLAAD-00N was open to air conversion into the fully reoxidized flavin spectrum required ≈ 20 min, suggesting a very limited dioxygen reactivity of reduced PmaLAAD-00N. Mixing the photoreduced membrane-devoid PmaLAAD-00N with buffer solutions equilibrated with increasing O_2 concentrations in the stopped-flow device (5-50% oxygen saturation, final concentration) did not yield to the reoxidized form of the flavin cofactor, as instead normally observed for flavooxidases (27), *i.e.* molecular dioxygen does not reoxidize $FADH_2$ bound to the enzyme in the time of measurement (≈ 2 min).

A complete reoxidation of membrane-free fully photoreduced PmaLAAD-00N was instead observed by adding benzyl viologen in the absence of light (Fig. 4*G*). In the presence of membranes, the photoreduced PmaLAAD-00N added of benzyl viologen is, at first, slightly reoxidized but then becomes again fully reduced (after 75 min in the absence of light, Fig. 4*H*). The latter experiment confirms the existence in *E. coli* membranes of an electron transfer from PmaLAAD to cytochrome b, as observed for anaerobic substrate reduction experiments (see above).

The activity of purified, membrane-devoid PmaLAAD-00N was also detected using artificial electron acceptors, such as indigotetrasulfonate, gallocyanine, 2,6-dichlorophenolindophenol, cytochrome c and nitroblue tetrazolium. The highest activity was apparent with 2,6-dichlorophenolindophenol (E_m = 217 mV at pH 7.5): specific activity was 8-fold higher compared to the value determined with oxygen only.

Production and Properties of the Soluble PmaLAAD-01N Variant—In order to design a soluble form of PmaLAAD (*i.e.* not associated to membranes) suitable for structural studies, the RONN server was used (30). This analysis shows two high disordered regions: from residues 1 to 50, encompassing a putative transmembrane α-helix (residues 8-28) predicted by Topcons (31), and from 450 to the C-terminal end of the protein (Fig. 1*A*). Based on the above predictions, two deletion variants were designed, starting from Met28 (PmaLAAD-01N) and Ala50 (PmaLAAD-02N), respectively. Both variants were produced with an additional HisTag sequence at the N-terminus (Fig. 1): the PmaLAAD-02N variant was not studied in details because of its low stability.

The PmaLAAD-01N variant, lacking the putative transmembrane α-helix, was expressed following the same protocol used for PmaLAAD and PmaLAAD-00N and was purified by HiTrap chelating affinity chromatography. PmaLAAD-01N is almost completely soluble: ≈ 25 mg of pure PmaLAAD-01N were purified from 1 L of culture with a > 95% purity. The enzymatic activity of the pure PmaLAAD-01N preparation was below detection both in the presence and in absence of *E. coli* membranes.

PmaLAAD-01N possesses an absorbance spectrum very similar to PmaLAAD-00N, with an estimated molar extinction coefficient at 458 nm of 12193 $M^{-1}cm^{-1}$ (Fig. 4*A*). On the contrary, circular dichroism far-UV spectrum of PmaLAAD-01N differs from the one recorded for the PmaLAAD-00N counterpart, showing a decrease in α-helix content (not shown).

When analysed by gel-permeation chromatography, purified PmaLAAD-00N and -01N variants eluted in a single peak corresponding to a molecular mass of ≈ 47 kDa and ≈ 44 kDa, respectively (slightly lower than the expected values of 52.4 kDa and 49.9 kDa), thus indicating that both variants are monomeric in solution in the 1-5 mg/mL protein concentrations.

Similarly to PmaLAAD-00N, PmaLAAD-

01N did not bind benzoate and did not react with sulfite, while interacted with anthranilate yielding a spectral perturbation which resembles a charge-transfer complex (K_d = 36.7 ± 5.6 mM, Fig. 4*D*). PmaLAAD-01N was also titrated with 2-aminobenzaldehyde: binding of this compound resulted into a large spectral change in the 500-580 nm range (K_d of 0.31 ± 0.05 mM, Fig. 4*F*).

When purified PmaLAAD-01N was mixed under anaerobic conditions with an excess of substrate (25 mM L-Phe), the FAD cofactor rapidly converted into the reduced form. Analogously to what was observed for PmaLAAD-00N, anaerobic reduction with stoichiometric amounts of L-Phe (1:1 or 1:2 enzyme:L-Phe ratios) in the absence of membranes resulted into a slow (6 or 5 hours, respectively) and partial reduction of FAD (not shown). Photoreduction of the FAD cofactor was fully accomplished after ≈ 10 min of illumination (with large amount of anionic semiquinone formation) and fully reverted to the oxidized form by mixing the photoreduced enzyme with benzyl viologen.

Altogether, the main biochemical properties of soluble, deleted PmaLAAD-01N and its FAD reactivity resemble the ones of the full-length enzyme.

Overall Structure of PmaLAAD-01N—The PmaLAAD-01N was solved at 2.0 Å resolution and refined to final R-factor and R-free of 16.6% and 21.1%, respectively. Data collection and refinement statistics are reported in Table 1. PmaLAAD-01N consists of two domains: a FAD binding domain (Fbd: residues 40-100, 203-276, 413-474) similar to the glutathione reductase 2 family (32) and a substrate binding domain (Sbd: residues 28-39, 101-202, 277-412) (Fig. 5*A*).

The Fbd is made up of a six-stranded β-sheet with β10-β3-β2-β14-β24-β23 topology flanked by a helix bundle formed by A1-A3-A6-A14 on one side and by a three-stranded β-sheet β11-β12-β13 and helix A7 on the other side. The C-terminal A15 and A16 helices (3_{10}) run orthogonal to strand β23 (Figs. 5B and S1). The helices A1 and A14 of the helix bundle pack against the central six-stranded β-sheet with their N-termini directed toward the FAD molecule. Helix A3 forms an outer layer of the fold, running orthogonally behind the A1, A6, and A14 helices. On the same side, the 3_{10} helix A2 flanks the pyrophosphate group of FAD. On the other side, the N-terminus of helix A7 is directed toward the FAD molecule.

The Sbd consists of a mixed eight-stranded β-sheet with β7-β8-β6-β16-β17-β18-β15-β22 topology and is flanked by helices A4, A5, A12 and the 3_{10} helix A13. The long β15 and β22 strands connect the Sbd and the Fbd, forming a four-stranded mixed β-sheet with β19 and β20. Another connection between the two domains is provided by strands β4 and β9 that form with strand β5 a small antiparallel three-stranded β-sheet (Fig. 5*B*).

The Sbd is characterized by the presence of a long region of 67 amino acids nestled between strand β19 and helix A12: this subdomain shows an α+β structure whose arrangement is unprecedented, as suggested by a DALI search (33). The α region consists of four helices: A8, A9, A10, and A11; the β-region includes strand β20, which forms a parallel two-stranded β-sheet with β19 from the core of the Sbd, and an antiparallel two-stranded β-sheet built up by strand β1 and β21. In particular, strand β1 belongs to the N-terminal region of PmaLAAD-01N (residues 28-39), which crosses the subdomain on the protein surface before inserting in the Fbd (Fig. 5*A*,*B*).

Regarding the quaternary assembly, the two PmaLAAD-01N molecules in the crystal asymmetric unit face each other in the Sbd regions corresponding to the end of A3 and the following loop, to A4-β7-A5, to A6 and to β16-β17. The facing residues (25 in each monomer) make six salt bridges and two H-bonds (distances 3-3.5 Å). According to the program PISA (34) these interactions make the complex stable, but the overall buried surface area is modest, ≈ 700 Å^2 for each monomer corresponding to ≈ 4% of the total surface accessible area. Thus, in agreement with gel permeation experiments, the PmaLAAD-01N does not show any quaternary architecture and can be considered monomeric.

Structural Relatives—A DALI analysis (33) indicates that PmaLAAD-01N tertiary structure resembles that of a series of FAD-binding oxidoreductases, such as the β subunit of L-proline dehydrogenase from *Pyrococcus horikoshii* (PDB code 1Y56; DALI Z-score of 42.3, residue identity of 23%) (35), glycine oxidase from *Bacillus subtilis* (PDB code 1C0I; DALI Z-score of 41.2, residue identity of 21%) (36), and the heterotetrameric sarcosine oxidase from *Corynebacterium* sp. U-96. (PDB code 3ADA; DALI Z-score of 40.9, residue identity of 23%) (37) and from *Stenotrophomonas maltophilia* (PDB code 2GAG; DALI Z-score of

40.2, residue identity of 23%) (18) (Table 4).

The structural relationship among all these proteins extends to an excellent conservation of tertiary structure, with a r.m.s. deviation ranging from 2.0 to 2.2 Å. The structural homology is particularly marked for the isolated Fbd, with a r.m.s. deviation in the 1.2-1.3 Å range, while for the isolated Sbd ranges from 1.9 to 2.2 Å (Table 4). Although the general correspondence of secondary structure elements is maintained in both domains (Fig. 5*C*), the orientation of the Sbd is slightly different if the Fdb is used for the structural superimposition (Fig. 6*A*). Most importantly, the additional α+β subdomain present in PmaLAAD-01N (Fig. 5*C*) is absent as such in the other relative proteins, with the first 20 N-terminal residues of PmaLAAD-01N either absent in 1Y56 and in 1C0I, or differently oriented if compared to the N-terminal region of 3ADA and 2GAG (Fig. 6*B*). We cannot exclude that the absence of the anchorage N-terminal helix in PmaLAAD-01N, as compared to the full-length enzyme, could affect the conformation of the following region.

FAD Binding Site—FAD binds to PmaLAAD-01N in an extended conformation similar to that found in related FAD binding proteins (32). Forty-three residues are directly involved in FAD binding (distances below 4.5 Å), sixteen of which establish electrostatic or polar interactions with the cofactor. Only five of the latter interactions involve side-chain atoms (residues Glu85, Lys86, Gln93, Ser94, Thr442), the others being due to main-chain atoms. The N-terminal ends of the helix dipole of A14 and of A1 are pointed toward the O2 position of the isoalloxazine ring, and toward the pyrophosphate group of FAD, respectively. These two dipoles are typical of GR2 family members.

Overall, the isoalloxazine ring is quite solvent exposed, especially at the N5 reactive site, located at the interface between the Fdb and the Sbd. It establishes hydrogen bonds with the N atom of Met441 and the N and OG1 atoms of Thr442 (FAD O2 atom), the N atoms of Ser99 and Gln100 (FAD O4 atom), and the N atom of Tyr98 (FAD N5 atom) while displaying van der Waals interactions with Gln93, Arg96, Ala97, Tyr98, Ser99, Gln100, Leu279, Gln281, Ala410, Val411, Val412, Val438, Trp439, Gly440, Met441, and Thr442 side chains. The FAD O4 atom is further hydrogen bonded to a water molecule located inside the active site cavity (Fig. 7*A*).

Furthermore, the model of PmaLAAD-01N in complex with N5-sulfo-FAD (generated on the basis of the isoalloxazine ring of a N5-sulfo-flavin mononucleotide, PDB code 1QCW) shows that the close vicinity of the PmaLAAD-01N helical A2 segment to the FAD N5 reactive site would provide steric clash of the bound sulfite with the A2-β4 loop (Fig. 7*B*), thus preventing sulfite binding (see above). In addition, the lack of such peculiar feature of flavooxidases is also supported by the absence of positively charged groups in proximity of the N1-C2=O locus of the isoalloxazine ring, whose presence would inductively promote the process: in PmaLAAD a partial positive charge may be only provided by the dipole associated to the N-terminus of the nearby helix A14.

Substrate Binding Site—In order to gain structural insight into the substrate-binding mode of the enzyme, the 3D structure of PmaLAAD-01N in complex with anthranilate (possessing both a carboxyl and an amino group, thus mimicking L-amino acids) was determined at 1.75 Å resolution (R_{factor} = 13.4%, R_{free} = 19.4%). Data collection and refinement statistics are reported in Table 1. The analysis of the calculated electron density map showed the substrate-analogue bound nearby the FAD isoalloxazine moiety (Fig. 8*A*).

Binding of anthranilate does not alter the PmaLAAD-01N global tertiary structure (r.m.s. deviation range 0.43-0.59 Å between complex and native structures, depending on the superimposed protein chains), nor promote quaternary assembly variation. Local differences in the backbone conformation are, however, evident in the β18-β19 loop, in helix A9 and the following loop (Fig. 8*A*). In particular helix A9, which is a 3_{10} helix in the protein, undergoes to reorganization being a regular α-helix in the PmaLAAD-01N/anthranilate complex. Notably, this region is part of the PmaLAAD-01N specific α+β subdomain and is located at the entrance of the substrate binding pocket.

Such entrance is unusually wide (15-20 Å, calculated from the Cα position of residues located on opposite sides of the entrance) and mainly negatively charged (Glu109, Asp145, Asp150, Glu154, Glu341, Asp417, Glu418) (Fig. 8*F*). The substrate binding pocket is deep (≈ 20 Å) and mostly hydrophobic; the anthranilate aromatic ring is stacked to the FAD isoalloxazine ring, at ≈ 4 Å distance, and located in a pocket lined by Leu279, Phe318, Val412, Val438, Trp439. The ligand carboxyl group is H-bonded to the NE and NH_2 atoms of Arg316 side-chain

(2.8 Å and 3.2 Å, respectively), to the NE2 atom of Gln100 side-chain (2.8 Å), and to the FAD O4 atom (3.3 Å), while the 2-amino group of the ligand is H-bonded to the carbonyl oxygen of Val438 (3.2 Å). Upon ligand binding, Arg316 changes dramatically its conformation to insert its side-chain into the active site and to H-bonding, together with Gln100, anthranilate at the *re* side of the isoalloxazine ring (Fig. 8*A*,*B*). Additionally, also Phe318 changes rotamer, orienting its side-chain parallel to the ligand aromatic ring, at ≈ 5 Å distance, and the structural changes occurring in the 316-318 region are transmitted to the adjacent 333-343 region, which is located at the entrance of the substrate binding pocket (Fig. 8*A*,*B*).

The PmaLAAD-01N/anthranilate complex is well suited to analyze the binding mode of L-Phe (Fig. 8*C*). The PmaLAAD-01N enzymatic activity recorded on the unnatural amino acid L-Phe ethylester (33% in comparison with L-Phe) finds its structural explanation in the presence of a pocket lined by Tyr98, Ala314 and Arg316, where the ethylester moiety of the substrate can nicely fit (Fig. 8*D*). On the contrary, binding of the D-isomer of Phe would instead result in a steric clash between its aromatic side-chain and the FAD isoalloxazine moiety (Fig. 8*E*), in keeping with the absence of activity assayed for D-amino acids.

DISCUSSION

PmaLAAD is a FAD-containing enzyme which catalyzes the stereoselective deamination of L-amino acids into the corresponding α-keto acids and ammonia without hydrogen peroxide formation, thus differing from known LAAOs. PmaLAAD shows a broad substrate specificity with a preference for neutral, aromatic L-amino acids: the highest activity is apparent for L-Phe, L-Leu, L-Met and L-Trp (Table 2). This agrees with the size and microenvironment of the substrate binding pocket which is lined by hydrophobic residues (Fig. 8*B*).

Subcellular fractionation and deletion of N-terminus sequences demonstrated that PmaLAAD is anchored to the membrane through a putative transmembrane α-helix (residues 8-28). The cellular localization is fundamental for the enzyme functionality: accordingly, PmaLAAD is fully active in the presence of membranes only. The purified full-length, membrane-devoid enzyme is practically inactive and the catalytic competence is acquired by adding crude *E. coli* membranes, while is only marginally increased using purified *E. coli* lipid extracts (Table 3). These results indicate that PmaLAAD needs a specific membrane partner for its activity, rather than the hydrophobic environment of the membrane. We suggest that the physiological partner for PmaLAAD could be cytochrome b, a membrane protein that accepts electrons from different donors (29). The two charged regions at the entrance of the substrate binding site, *i.e.* the negatively and the positively charged regions shown in Fig. 8*F*, as well as the α+β subdomain, might play a major role in recognizing interacting protein(s) involved in the electron-transfer process.

The electron transfer from reduced PmaLAAD to membrane-bound electron acceptor(s) might also be responsible for the O_2-consumption observed when the enzymatic activity was assayed in the presence of membranes. The substrate-reduced or photoreduced purified PmaLAAD slowly reoxidized on dioxygen, as instead observed for both DAAOs and LAAOs (4,26,38). Reactivity of flavoproteins toward molecular oxygen was related to the microenvironment of the isoalloxazine ring, in particular to the presence of positively charged residues in proximity of the C4a position, e.g. Lys326 on the *si* face of the flavin in LAAO from snake venom or two histidines on the *re* face of FAD in glucose oxidases (39,40). The corresponding positions in the vicinity of the isoalloxazine moiety of FAD in PmaLAAD are instead occupied by the neutral Gln281 and the hydrophobic residues Trp439 and Val438. The lack of O_2-reoxidation of $FADH_2$ in PmaLAAD explains its inability to produce hydrogen peroxide and classifies it outside the oxidase class of flavoenzymes (27), which members represent the most close structural relatives (Fig. 5*C* and Fig. 6).

The FAD cofactor is bound in an extended conformation and establishes a high number of interactions with PmaLAAD apoprotein, comprising the interaction of helix dipole A14 with the O2 of the isoalloxazine ring (Fig. 7*A*) that is expected to stabilize the anionic form of $FADH_2$. The isoalloxazine ring is located at the interface between the substrate and FAD binding domains and is solvent exposed, especially at the N5 site: its location is compatible with electron transfer to the bound acceptor protein.

The overall fold of PmaLAAD resembles the one of known amine or amino acid oxidases/dehydrogenases (Fig. 6) but with specific structural features that allow to fulfil a

different role, *i.e.* the deamination of L-amino acid to fuel the membrane electron-transfer chain. Indeed, phylogenetic analysis demonstrates that proteins highly homologous to PmaLAAD (≥ 28% sequence identity) are present only in the Proteobacteria phylum, and in particular in the subphyla of alpha-, beta- and gamma-proteobacteria (Fig. 9). Noteworthy, all related sequences belongs to putative flavoprotein oxidases or deaminases with unknown function while the sequence identity with known microbial DAAOs or LAAOs is quite low (*i.e.* between 13.9% and 16.4%). This suggests that LAADs diverged early from amino acid oxidases but conserved a similar active site organization related to the use of the same substrate. In common with known amino acid oxidases, PmaLAAD shows a similar overall fold, the ability to generate the anionic semiquinone form of FAD during photoreduction, and the production of charge-transfer complexes following binding of carboxylic acids. At difference from these well-known flavooxidases, PmaLAAD shows an additional α+β subdomain (probably involved in recruiting the electron-acceptor partner), a solvent exposed FAD isoalloxazine ring and the inability of the reduced flavin to efficiently react with dioxygen and thus to produce hydrogen peroxide. Interestingly, comparison of the free and anthranilate bound structures of PmaLAAD-01N shows that part of the active site, in particular Arg316 (which binds the carboxyl group of substrate) and Phe318 (which forms hydrophobic interactions with the apolar moiety of the ligand), acquires a correct geometry only in the presence of the substrate (Fig. 8A). This behavior is not observed in classical flavoprotein oxidases such as DAAOs or LAAOs (4,38,41).

In summary, we set-up a procedure to prepare a stable PmaLAAD preparation (containing membrane fragments) that can be employed in cell-free biocatalysis, demonstrated that purified PmaLAAD can use electron-acceptors alternative to O_2 or cytochrome b (*i.e.* 2,6-dichlorophenolindophenol), and solved for the first time the 3D structure of a soluble form of this enzyme. Altogether these results provide the bases to push protein engineering studies aimed to manipulate LAAD substrate specificity in order to fulfill different biotechnological requests, such as the resolution of racemic mixtures of natural and unnatural amino acids or the generation of novel synthetic biochemical pathways (1,42).

Acknowledgements: The gene encoding for LAAD from *P. myxofaciens* was a generous gift of Wolfgang Kroutil (University of Graz).

Conflict of interest: The authors declare that they have no conflicts of interest with the contents of this article.

Author contributions: PM and GM performed biochemical experiments, analysed the experimental data and wrote the manuscript. MN performed the crystallization trials, solved the 3D structure and wrote the manuscript. LP designed experiments, analysed the data and wrote the manuscript.

REFERENCES

1. Turner, N. J. (2004) Enzyme catalysed deracemisation and dynamic kinetic resolution reactions. *Curr. Opin. Chem. Biol.* **8**, 114-119
2. Pollegioni, L., and Molla, G. (2011) New biotech applications from evolved D-amino acid oxidases. *Trends Biotechnol.* **29**, 276-283
3. Pollegioni, L., Sacchi, S., Caldinelli, L., Boselli, A., Pilone, M.S., Piubelli, L., and Molla, G. (2007) Engineering the properties of D-amino acid oxidases by a rational and a directed evolution approach. *Curr. Protein Pept. Sci.* **8**, 600-618
4. Pollegioni, L., Motta, P., and Molla, G. (2013) L-amino acid oxidase as biocatalyst: a dream too far? *Appl. Microbiol. Biotechnol.* **97**, 9323-9341
5. Pantaleone, D. P., Geller, A. M., and Taylor, P. P. (2001) Purification and characterization of an L-amino acid deaminase used to prepare unnatural amino acids. *J. Mol. Catal. B: Enzym.* **11**, 795-803
6. Busto, E., Richter, N., Grischek, B., and Kroutil, W. (2014) Biocontrolled formal inversion or retention of L-α-amino acids to enantiopure (R)- or (S)-hydroxyacids. *Chemistry* **20**, 11225-11228

7. Hou, Y., Hossain, G. S., Li, J., Shin, H. D., Liu, L., and Du, G. (2015) Production of phenylpyruvic acid from L-phenylalanine using an L-amino acid deaminase from *Proteus mirabilis*: comparison of enzymatic and whole-cell biotransformation approaches. *Appl. Microbiol. Biotechnol.* **99**, 8391-8402
8. Giammanco, G. M., Grimont, P. A., Grimont, F., Lefevre, M., Giammanco, G., and Pignato, S. (2011) Phylogenetic analysis of the genera *Proteus*, *Morganella* and *Providencia* by comparison of *rpoB* gene sequences of type and clinical strains suggests the reclassification of *Proteus myxofaciens* in a new genus, *Cosenzaea* gen. nov., as *Cosenzaea myxofaciens* comb. nov. *Int. J. Syst. Evol. Microbiol.* **61**, 1638-1644
9. Caldinelli, L., Sacchi, S., Molla, G., Nardini, M., and Pollegioni, L. (2013) Characterization of human DAAO variants potentially related to an increased risk of schizophrenia. *Biochim. Biophys. Acta* **1832**, 400-410
10. Volontè, F., Marinelli, F., Gastaldo, L., Sacchi, S., Pilone, M. S., Pollegioni, L., and Molla, G. (2008) Optimization of glutaryl-7-aminocephalosporanic acid acylase expression in *E. coli*. *Protein Expr. Purif.* **61**, 131-137
11. Molla, G., Piubelli, L., Volontè, F., and Pilone, M. S. (2012) Enzymatic detection of D-amino acids. *Methods Mol. Biol.* **794**, 273-289
12. Harris, C. M., Pollegioni, L., and Ghisla, S. (2001) pH and kinetic isotope effects in D-amino acid oxidase catalysis. *Eur. J. Biochem.* **268**, 5504-5520
13. Molla, G., Porrini, D., Job, V., Motteran, L., Vegezzi, C., Campaner, S., Pilone, M. S., and Pollegioni, L. (2000) Role of arginine 285 in the active site of *Rhodotorula gracilis* D-amino acid oxidase. A site-directed mutagenesis study. *J. Biol. Chem.* **275**, 24715-24721
14. Harris, C. M., Molla, G., Pilone, M. S., and Pollegioni, L. (1999) Studies on the reaction mechanism of *Rhodotorula gracilis* D-amino-acid oxidase. Role of the highly conserved Tyr-223 on substrate binding and catalysis. *J. Biol. Chem.* **274**, 36233-26240
15. Kabsch, W. (2010) XDS. *Acta Crystallogr. D Biol. Crystallogr.* **66**, 125-132
16. Evans, P. (2006) Scaling and assessment of data quality. *Acta Crystallogr. D Biol. Crystallogr.* **62**, 72-82
17. Storoni, L. C., McCoy, A. J., and Read, R. J. (2004) Likelihood-enhanced fast rotation functions. *Acta Crystallogr. D Biol. Crystallogr.* **60**, 432-438
18. Chen, Z. W., Hassan-Abdulah, A., Zhao, G., Jorns, M. S., and Mathews, F. S. (2006) Heterotetrameric sarcosine oxidase: structure of a diflavin metalloenzyme at 1.85 Å resolution. *J. Mol. Biol.* **360**, 1000-1018
19. Adams, P. D., Afonine, P. V., Bunkóczi, G., Chen, V. B., Davis, I. W., Echols, N., Headd, J. J., Hung, L. W., Kapral, G. J., Grosse-Kunstleve, R. W., McCoy, A. J., Moriarty, N. W., Oeffner, R., Read, R. J., Richardson, D. C., Richardson, J. S., Terwilliger, T. C., and Zwart, P. H. (2010) PHENIX: a comprehensive Python-based system for macromolecular structure solution. *Acta Crystallogr. D Biol. Crystallogr.* **66**, 213-221
20. Emsley, P., and Cowtan, K. (2004) Coot: model-building tools for molecular graphics. *Acta Crystallogr. D Biol. Crystallogr.* **60**, 2126-2132
21. Murshudov, G. N., Vagin, A. A., and Dodson, E. J. (1997) Refinement of macromolecular structures by the maximum-likelihood method. *Acta Crystallogr. D Biol. Crystallogr.* **53**, 240-255
22. Chen, V. B., Arendall 3rd, W. B., Headd, J. J., Keedy, D. A., Immormino, R. M., Kapral, G. J., Murray, L. W., Richardson, J. S., and Richardson, D. C. (2010) MolProbity: all-atom structure validation for macromolecular crystallography. *Acta Crystallogr. D Biol. Crystallogr.* **66**, 12-21
23. Baek, J. O., Seo, J. W., Kwon, O., Seong, S. I., Kim, I. H., and Kim, C. H. (2011) Expression and characterization of a second L-amino acid deaminase isolated from *Proteus mirabilis* in *Escherichia coli*. *J. Basic Microbiol.* **51**, 129-135
24. Fonda, M. L., and Anderson, B. M. (1968) D-amino acid oxidase. II. Studies of substrate-competitive inhibitors. *J. Biol. Chem.* **243**, 1931-1935
25. Sacchi, S., Caldinelli, L., Cappelletti, P., Pollegioni, L., and Molla, G. (2012) Structure-function relationships in human D-amino acid oxidase. *Amino Acids* **43**, 1833-1850
26. Pollegioni, L., Langkau, B., Tischer, W., Ghisla, S., and Pilone, M. S. (1993) Kinetic mechanism of D-amino acid oxidases from *Rhodotorula gracilis* and *Trigonopsis variabilis*. *J. Biol. Chem.* **268**, 13850-13857
27. Massey, V., and Hemmerich, P. (1980) Active-site probes of flavoproteins. *Biochem. Soc. Trans.*

8, 246-257
28. Volbeda, A., Darnault, C., Parkin, A., Sargent, F., Armstrong, F. A., and Fontecilla-Camps, J. C. (2012) Crystal structure of the O(2)-tolerant membrane-bound hydrogenase 1 from *Escherichia coli* in complex with its cognate cytochrome b. *Structure* **21**, 184-190.
29. van Wielink, J. E., Reijnders, W. N., Oltmann, L. F., and Stouthamer, A. H. (1983) Electron transport and cytochromes in aerobically grown *Proteus mirabilis*. *Arch. Microbiol.* **136**, 152-157
30. Yang, Z. R., Thomson, R., McNeil, P., and Esnouf, R. M. (2005) RONN: the bio-basis function neural network technique applied to the detection of natively disordered regions in proteins. *Bioinformatics* **21**, 3369-3376
31. Bernsel, A., Viklund, H., Hennerdal, A., and Elofsson, A. (2009) TOPCONS: consensus prediction of membrane protein topology. *Nucleic. Acids Res.* **37**, W465-W468
32. Dym, O., and Eisenberg, D. (2001) Sequence-structure analysis of FAD-containing proteins. *Protein Sci.* **10**, 1712-1728
33. Holm, L., and Rosenström, P. (2010) Dali server: conservation mapping in 3D. *Nucl. Acids Res.* **38**, W545-W549
34. Krissinel, E., and Henrick, K. (2007) Inference of macromolecular assemblies from crystalline state. *J. Mol. Biol.* **372**, 774-797
35. Tsuge, H., Kawakami, R., Sakuraba, H., Ago, H., Miyano, M., Aki, K., Katunuma, N., and Ohshima, T. (2005) Crystal structure of a novel FAD-, FMN-, and ATP-containing L-proline dehydrogenase complex from *Pyrococcus horikoshii*. *J. Biol. Chem.* **280**, 31045-31049
36. Mörtl, M., Diederichs, K., Welte, W., Molla, G., Motteran, L., Andriolo, G., Pilone, M. S., and Pollegioni, L. (2004) Structure-function correlation in glycine oxidase from *Bacillus subtilis*. *J. Biol. Chem.* **279**, 29718-29727
37. Moriguchi, T., Ida, K., Hikima, T., Ueno, G., Yamamoto, M., and Suzuki, H. (2010) Channeling and conformational changes in the heterotetrameric sarcosine oxidase from *Corynebacterium* sp. U-96. *J. Biochem.* **148**, 491-505
38. Pawelek, P. D., Cheah, J., Coulombe, R., Macheroux, P., Ghisla, S., and Vrielink, A. (2000) The structure of L-amino acid oxidase reveals the substrate trajectory into an enantiomerically conserved active site. *EMBO J.* **19**, 4204-4215
39. Mattevi, A. (2006) To be or not to be an oxidase: challenging the oxygen reactivity of flavoenzymes. *Trends Biochem. Sci.* **31**, 276-283
40. Saam, J., Rosini, E., Molla, G., Schulten, K., Pollegioni, L., and Ghisla, S. (2010) O_2 reactivity of flavoproteins: dynamic access of dioxygen to the active site and role of a H^+ relay system in D-amino acid oxidase. *J. Biol. Chem.* **285**, 24439-24446
41. Umhau, S., Pollegioni, L., Molla, G., Diederichs, K., Welte, W., Pilone, M. S., and Ghisla, S. (2000) The X-ray structure of D-amino acid oxidase at very high resolution identifies the chemical mechanism of flavin-dependent substrate dehydrogenation. *Proc. Natl. Acad. Sci. USA* **97**, 12463-12468
42. Tessaro, D., Pollegioni, L., Piubelli, L., D'Arrigo, P., and Servi, S. (2015) Systems Biocatalysis: An Artificial Metabolism for Interconversion of Functional Groups. *ACS Catal.* **5**, 1604-1608
43. Finn, R. D., Clements, J., and Eddy, S. R. (2011) HMMER web server: interactive sequence similarity searching. *Nucleic Acids Res.* **39**, W29-W37
44. Chen, C., Natale, D. A., Finn, R.D., Huang, H., Zhang, J., Wu, C.H., and Mazumder, R. (2011) Representative proteomes: a stable, scalable and unbiased proteome set for sequence analysis and functional annotation. *PLoS One* **6**, e18910
45. Huang, Y., Niu, B., Gao, Y., Fu, L., and Li, W. (2010) CD-HIT Suite: a web server for clustering and comparing biological sequences. *Bioinformatics* **26**, 680-682
46. Gouy, M., Guindon, S., and Gascuel, O. (2010) SeaView version 4: A multiplatform graphical user interface for sequence alignment and phylogenetic tree building. *Mol. Biol. Evol.* **27**, 221-224
47. Guindon, S., Dufayard, J. F., Lefort, V., Anisimova, M., Hordijk, W., and Gascuel, O. (2010) New algorithms and methods to estimate maximum-likelihood phylogenies: assessing the performance of PhyML 3.0. *Syst. Biol.* **59**, 307-321
48. Felsenstein, J. (1985) Confidence limits on phylogenies: an approach using the bootstrap. *Evolution* **39**, 783-791

FOOTNOTES
This work was supported by a grant from Fondo di Ateneo per la Ricerca to GM and LP. PM is a PhD student of the Degree in Analysis, Protection and Management of Biodiversity at the Università degli Studi dell'Insubria.

The abbreviations used are: AT, aminotransferase; DAAO, D-amino acid oxidase; Fbd, FAD binding domain; MPD, 2-Methyl-2,4-pentanediol; LAAD, L-amino acid deaminase; LAAO, L-amino acid oxidases; PmaLAAD, L-amino acid deaminase from *Proteus myxofaciens*; PmaLAAD-00C, C-terminal His-tagged PmaLAAD; PmaLAAD-00N, N-terminal His-tagged PmaLAAD; PmaLAAD-01N, truncated PmaLAAD-00N starting from Met28; PmaLAAD-02N, truncated PmaLAAD-00N starting from Ala50; Sbd, substrate binding domain.

FIGURE LEGENDS

FIGURE 1. **Amino acid sequence of PmaLAAD variants produced in this work.** *A*, scheme of produced PmaLAAD variants showing the predicted disordered regions and putative transmembrane α-helix. *B*, sequence comparison of produced PmaLAAD variants; residues are numbered as in PmaLAAD wild type. Black and grey boxes: HisTag and GXGXXG sequences, respectively. PmaLAAD-00N possesses nine and PmaLAAD-00C eight additional residues as compared to PmaLAAD wild type.

FIGURE 2. **Purification scheme of recombinant PmaLAAD from *E. coli* cells.** Because of the impossibility to fractionate PmaLAAD by chromatographic techniques, the best purification was obtained by ultracentrifugation of the crude extract of *E. coli* cells expressing PmaLAAD and re-suspending the pellet in 50 mM potassium phosphate buffer, pH 7.5. Values reported in grey boxes represent actual values obtained from a 120 mL culture (0.41 g cells) purification.

FIGURE 3. **Apparent kinetic parameters on L-Phe and pH and temperature dependence of the activity of PmaLAAD.** *A*, enzymatic activity was determined at air saturation by the increase of the product phenylpyruvate. Data points were fitted with an hyperbolic equation. *B*, activity of PmaLAAD at 25 °C at the indicated pH values in multicomponent buffer (12). Data are expressed as percentage of maximal enzyme activity. Data points were fitted based on the equation for two dissociations: $Y = a + b(10^{pH-pKa1}) / (1 + 10^{pH-pKa1}) + [b - c(10^{pH-pKa2}) / (1 + 10^{pH-pKa2})]$ (14); estimated pK_{a1} was 5.8 ± 0.1 and pK_{a2} was 8.3 ± 0.3. *C*, activity of PmaLAAD determined at the indicated temperatures. Data are expressed as percentage of enzyme activity assayed at 50 °C (the maximum value). In panels *B* and *C*, activity was determined on 25 mM L-Phe at pH 7.5. For each assay 10 µL (corresponding to 25 µg of enzyme) of resuspended membrane containing PmaLAAD fraction was used.

FIGURE 4. **Spectral properties of PmaLAAD-00N and PmaLAAD-01N variants.** *A*, absorbance spectrum of PmaLAAD-00N in the oxidized and reduced form, obtained by anaerobic addition of 25 mM L-Phe (full line), and of PmaLAAD-01N (dashed line) in the oxidized form. *B*, absorbance spectrum of 17 µM PmaLAAD-00N in the oxidized and reduced form (dotted line) by anaerobic addition of 25 mM L-Phe in the presence of *E. coli* membranes. Dashed line represents the spectral species obtained after the first (faster and wider) reduction phase (see main text). *C*, *D*, binding of anthranilate to 15 µM PmaLAAD-00N and 14.6 µM PmaLAAD-01N, respectively. Selected spectra obtained upon addition of increasing concentrations of anthranilate are shown. *E*, binding of kojic acid to 15 µM PmaLAAD-00N; selected spectra obtained upon addition of increasing ligand concentrations (up to 242 mM) are shown. *F*, binding of 2-aminobenzaldehyde (up to 10 mM) to PmaLAAD-01N variant. *g*, spectra recorded at different times during photoreduction of 20 µM PmaLAAD-00N; the maximal amount of reduced flavin species (dashed line) is detected after 5 min of photoillumination. The photoreduced enzyme was anaerobically mixed with benzyl viologen yielding the re-oxidized enzyme after 45 min of incubation (dotted line). *H*, spectra recorded at different times during photoreduction of 17 µM PmaLAAD-00N in the presence of *E. coli* membranes (from 280 mg of cells); the maximal amount of reduced flavin species (dashed line) was detected after 3.5 min of photoillumination. The photoreduced enzyme was then anaerobically mixed with benzyl viologen (dotted line). Bold line: spectrum of the original, oxidized enzyme. The arrows in panels indicate the direction of absorbance change at increasing ligand concentrations (panels *C-F*) or at different times (panels *G* and *G*). All insets: the observed increase in absorbance at selected wavelengths is plotted as a function of the ligand concentration: the solid line is a fit of the data to a hyperbolic binding curve. Spectra were recorded in 50 mM potassium phosphate, pH 7.5 and 15 °C.

FIGURE 5. **Crystal structure of PmaLAAD-01N, topology and structure-based sequence alignment.** *A*, schematic view of the domain spatial arrangement in PmaLAAD-01N. The FAD binding domain is in green (with the α+β additional subdomain in blue), the substrate binding domain in orange; α-helices, β -strands, and coils are represented by helical ribbons, arrows, and ropes, respectively. The FAD cofactor is shown in stick representation (yellow color). The N- and C-termini of PmaLAAD-01N are labelled. *B*, secondary structure topology diagram of PmaLAAD-01N: cylinders and arrows indicate helices and strands, respectively. *C*, structure-based sequence alignment of PmaLAAD-01N. PmaLAAD-01N is aligned with L-proline dehydrogenase from *Pyrococcus horikoshii* (PDB code

1Y56), glycine oxidase from *Bacillus subtilis* (PDB code 1C0I) and heterotetrameric sarcosine oxidases from Corynebacterium sp. U-96 (PDB code 3ADA) and from *Stenotrophomonas maltophilia* (PDB code 2GAG). The sequence alignment has been performed using the CLUSTALW program (http://www.ebi.ac.uk/Tools/msa/clustalw2/) and manually corrected based on their three-dimensional structure comparisons. PmaLAAD-01N secondary structure elements are shown on the top of the alignment and shaded in gray (yellow for 310 helices) for all aligned proteins. Asterisks and circles indicate PmaLAAD-01N residues interacting with the FAD, isoalloxazine ring and with anthranilate, respectively.

FIGURE 6. **Structural comparison with related proteins.** *A*, the structural comparison is produced by superimposing the FAD binding domains of PmaLAAD-01N (green, α+β subdomain blue) with L-proline dehydrogenase from Pyrococcus horikoshii (PDB code 1Y56, orange), or glycine oxidase from *Bacillus subtilis* (PDB code 1C0I, magenta), or heterotetrameric sarcosine oxidase from *Corynebacterium sp.* U-96 (PDB code 3ADA, cyan) and from *Stenotrophomonas maltophilia* (PDB code 2GAG, yellow). The FAD cofactor bound to the PmaLAAD-01N is shown in stick representation (green color). *B*, the different orientation of the N-terminus in PmaLAAD-01N relative to the heterotetrameric sarcosine oxidase from *Corynebacterium sp.* U-96 (PDB code 3ADA, cyan) and from *Stenotrophomonas maltophilia* (PDB code 2GAG, yellow) is shown. PmaLAAD-01N Leu52 is labelled to indicate the position where the backbone of the three proteins starts to show a good superimposition. In both panels the FAD cofactor bound to the PmaLAAD-01N FAD-binding domain is shown in stick representation (green color).

FIGURE 7. **Protein–isoalloxazine ring interactions and active site cavity of PmaLAAD-01N.** *A*, the FAD molecule (yellow) and the protein residues (green) located at the active site cavity relevant for FAD binding are shown in stick representation and labeled. A water molecule is represented as red sphere (0.3 vdW radius). H-bonds are shown by dashed lines. *B*, model of the N5-sulfo-FAD molecule bound to PmaLAAD-01N based on the isoalloxazine ring of a N5-sulfo-flavin mononucleotide molecule (PDB code 1QCW).

FIGURE 8. **Ligand binding to PmaLAAD-01N.** *A*, structural reorganization of the substrate binding pocket in PmaLAAD subunit B upon anthranilate binding. The bound anthranilate (ANT) is shown in stick representation (cyan) surrounded by its 2Fo-Fc electron density, contoured at 1σ (cyan mesh). The structure of the PmaLAAD-01N/anthranilate complex (color code as in Figure 5) is superimposed to the unbound PmaLAAD-01N (grey) to highligth the backbone differences in the regions 316-318 (the β18-β19 loop) and 333-343 (helix A9 and the following loop), and the side-chain structural variations of Arg316 and Phe318. *B*, substrate binding pocket in PmaLAAD-01N. The bound anthranilate, the FAD molecule and the relevant protein residues are shown in stick representation and labelled. Dashed lines indicate H-bonds. For clarity, the A9 region shown in panel A has been omitted. Modeling of the bound *C*, L-Phe, *D*, L-Phe ethylester, and *E*, D-Phe, based on the PmaLAAD-01N/anthranilate complex. *F*, entrance of the active site. Molecular surface of PmaLAAD-01N, colored according to its potential (blue positive, red negative). The entry of the active site cavity, showing the isoalloxazine ring of FAD (yellow) and the bound anthranilate (grey), is clearly visible.

FIGURE 9. **Phylogenetic analysis.** Proteins homologous to PmaLAAD (> 28% sequence identity) are only present in the *Proteobacteria* phylum, in particular in the subphyla of alphaproteobacteria, betaproteobacteria and gammaproteobacteria. Homologous proteins form three main clusters and an isolated sequence (B): a group close to PmaLAAD (LAAD) and two large groups (A and C). Noteworthy, all identified proteins are putative flavoprotein oxidases or deaminases with unknown function. Numbers on the branches represent the percentage of bootstrap samples supporting the branch (only values > 50% are shown). PmaLAAD is indicated by an arrow. Sequences are identified by their UniProtKB Accession Number. Proteins homologous to PmaLAAD were identified with HMMER web server (43) using the "Representative Proteomes" database (44). Sequences sharing an identity > 90% with PmaLAAD were filtered using CD-HIT Suite (45). In addition, amino acid sequences possessing an identity with PmaLAAD < 28% were discarded. Alignment was performed using MUSCLE algorithm in SeaView software (46). Maximum-likelihood phylogenetic (ML) tree of LAAD sequences

was built using PhyML 3.0 server (47). Confidence of branching patterns was assessed by bootstrapping (100 boostrap samples were used) (48). The resulting ML tree was visualized in FigTree v1.4.2 (http://tree.bio.ed.ac.uk/software/figtree/).

FIGURES AND TABLES

TABLE 1
Data collection and refinement statistics
Numbers given in parentheses are from the last resolution shell.

Data Collection	**PmaLAAD-01N**	**PmaLAAD-01N + anthranilate**
X-Ray source	ESRF ID23-2	ESRF ID23-1
Space group	$P2_1$	$P2_1$
Unit cell dimensions:		
a, b, c (Å)	72.76, 93.71, 74.69	72.81, 93.32, 75.07
α, β, γ (°)	90, 102.85, 90	90, 103.22, 90
Resolution (Å)	49.08-2.00 (2.11-2.00)	45.90-1.75 (1.84-1.75)
Observations	298242	257980
Unique reflections	65982	96409
R-merge (%)[a]	9.4 (51.4)	3.4 (51.3)
I/σ(I)	12.0 (2.9)	14.9 (1.9)
Completeness (%)	99.9 (99.9)	98.1 (97.9)
Multiplicity	4.5 (4.7)	2.7 (2.7)
Refinement		
R-factor/R-free (%)[b]	16.6/21.1	13.4/19.4
Protein residues in the a.u.	2x447 (28-474)	2x447 (28-474)
FAD	2	2
Anthranilic acid	-	2
Water molecules	520	537
Model quality		
Average B-factor (Å^2):		
Protein	26.6	39.0
FAD	16.2	23.7
ligand	-	44.5
water	31.5	45.6
Rmsd from ideal values:		
bond lengths (Å)	0.013	0.008
bond angles (°)	1.705	1.438
Ramachandran plot:		
most favored regions	96.3	96.6
additional allowed regions	3.7	3.4

[a] $R_{merge} = \Sigma_h\Sigma_i | I_{hi} - \langle I_h \rangle | / \Sigma_h\Sigma_i I_{hi}$
[b] $R_{factor} = \Sigma_h ||F_{obs}| - |F_{calc}|| / \Sigma_h |F_{obs}|$, with F_{obs} being the observed and F_{calc} the calculated structure factor amplitudes

TABLE 2

Relative specific activity of PmaLAAD on different substrates

The activity was determined by the polarographic assay (oxygen consumption) using a membrane-containing PmaLAAD preparation and 25 mM substrate concentration with the exception of L-Tyr (1.25 mM), β^3-Phe (12.5 mM), 1-naphthyl-Ala (0.375 mM) and Gly (0.375 mM). *Specific activity was expressed as percentage of the value assessed with L-Phe (100%). **The activity value for the corresponding D-amino acid was ≤ 4%. ***The activity on this compound was confirmed by using for the assay a purified (by re-crystallization) substrate batch to avoid contamination by residual free L-Phe.

Amino acid	Specific activity (%)*	Amino acid	Specific activity (%)*,**
Neutral:		Charged:	
Gly	0.06	L-Asp	0.13
L-Ala	0.59	L-Glu	0.11
L-Pro	0.96	L-His	9.88
L-Ile	26.2	L-Lys	3.45
L-Val	3.47	L-Arg	8.0
L-Leu	99.2**	Unnatural:	
L-Met	86.0**	β-Ala	0.21
Aromatic:		β^2-Phe	0.24
L-Phe	100**	β^3-Phe	0.06
L-Tyr	13.7	D,L-tert-Leu	0.99
L-Trp	60.5**	L-Phe amide	2.29
Polar:		L-Phe-O-ethyl ester***	33.0
L-Cys	43.0**	1-Naphtyl-Gly	0.58
L-Ser	0	1-Naphtyl-Ala	3.75
L-Thr	0.09	2-Amino octanoic acid	0
L-Asn	0.74	3-Phenyl-Ser	3.49
L-Gln	0.55	Glufosinate	0.54
		D,L- DOPA	0.57

TABLE 3

PmaLAAD-00N activity recovery with purified *E. coli* lipid extracts

The activity was determined by the polarographic assay (oxygen consumption) on 25 mM L-Phe as a substrate, using ≈ 150 μg of purified protein. All mixtures have been sonicated before the assay, until the solution appeared completely clear.

Sample	Activity (U/mL)	Increase (-fold)
PmaLAAD-00N (Control)	0.25 ± 0.06	1.0
PmaLAAD-00N + membranes from 45 mg cells	7.74 ± 0.37	31.5
PmaLAAD-00N + 4.5 mg Total Lipid extract	0.98 ± 0.13	4.0
PmaLAAD-00N + 4.5 mg Polar Lipid extract	0.39 ± 0.11	1.6
PmaLAAD-00N + membranes from 22.5 mg cells	3.45 ± 0.25	14.0
PmaLAAD-00N + membranes from 22.5 mg cells + 2.25 mg Total Lipid extract	4.96 ± 0.42	20.2
PmaLAAD-00N + membranes from 22.5 mg cells + 2.25 mg Polar Lipid extract	3.97 ± 0.15	16.1

TABLE 4

Structural comparison of proteins homologous to PmaLAAD-01N

PDB	chain	Z score	r.m.s. deviation			ali	nres	Id (%)	Protein	Ref.
			all	FbD	SbD					
1Y56	B	42.3	2.0 (361)	1.2 (179)	2.0 (174)	361	374	23	L-proline dehydrogenase complex from *Pyrococcus horikoshii*	(35)
1C0I	B	41.2	2.0 (353)	1.3 (176)	2.2 (171)	353	364	21	glycine oxidase from *Bacillus subtilis*	(36)
3ADA	B	40.9	2.2 (368)	1.3 (177)	1.9 (175)	368	397	23	heterotetrameric sarcosine oxidase from *Corynebacterium* sp. U-96.	(37)
2GAG	B	40.2	2.2 (368)	1.3 (176)	1.9 (176)	368	403	23	heterotetrameric sarcosine oxidase from *Stenotrophomonas maltophilia*	(18)

Figure 1

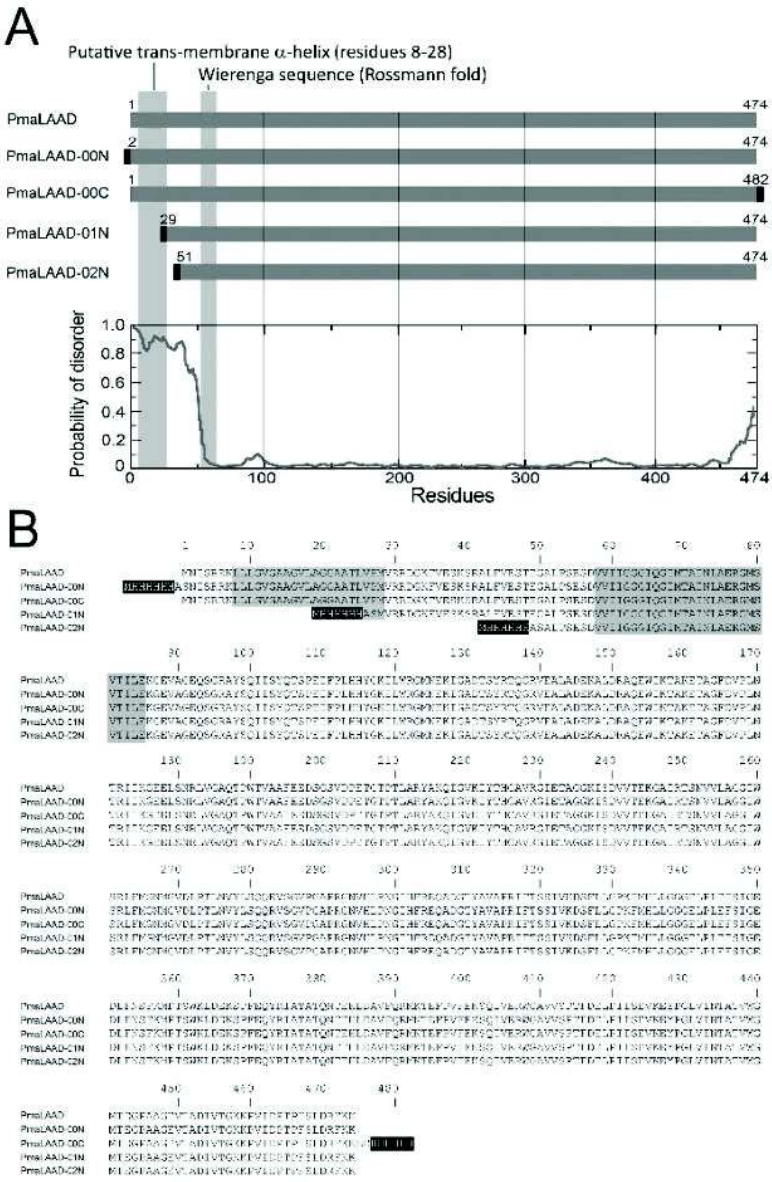

Figure 2

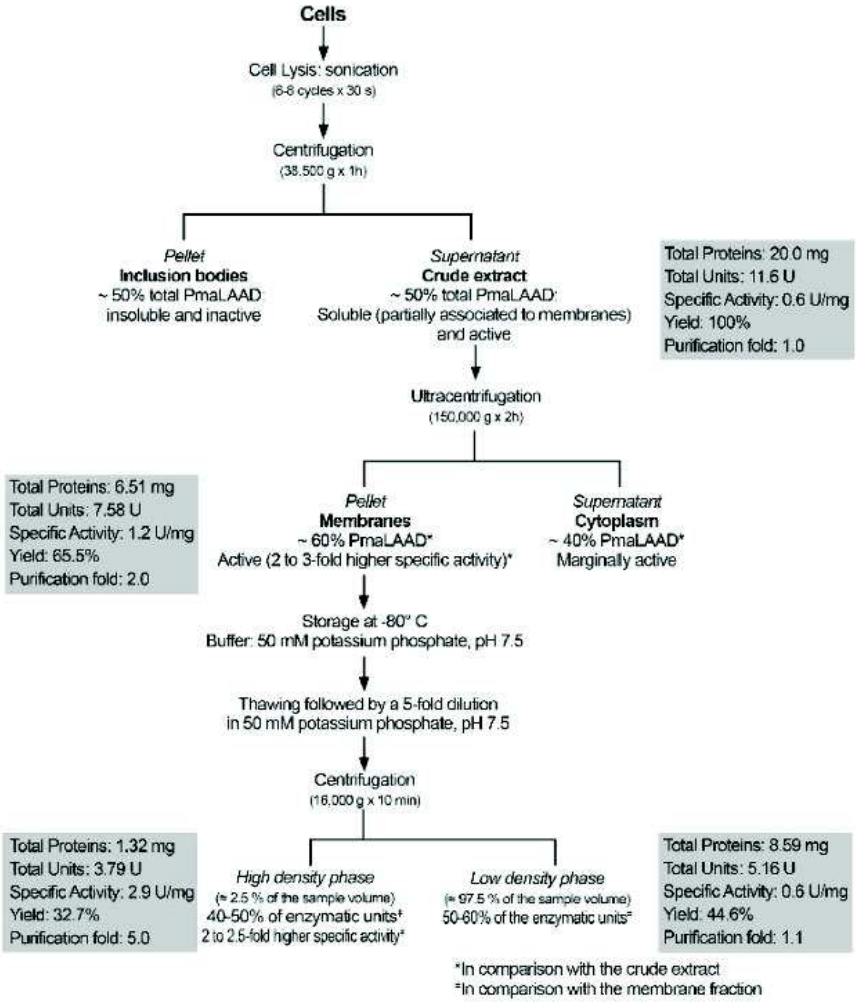

Figure 3

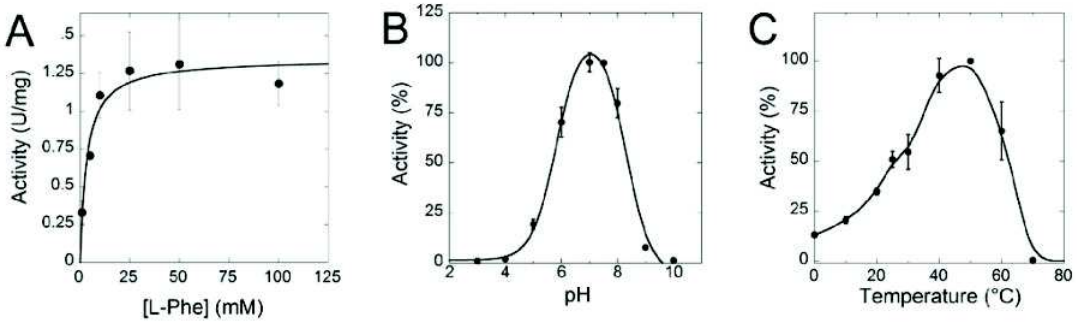

Figure 4

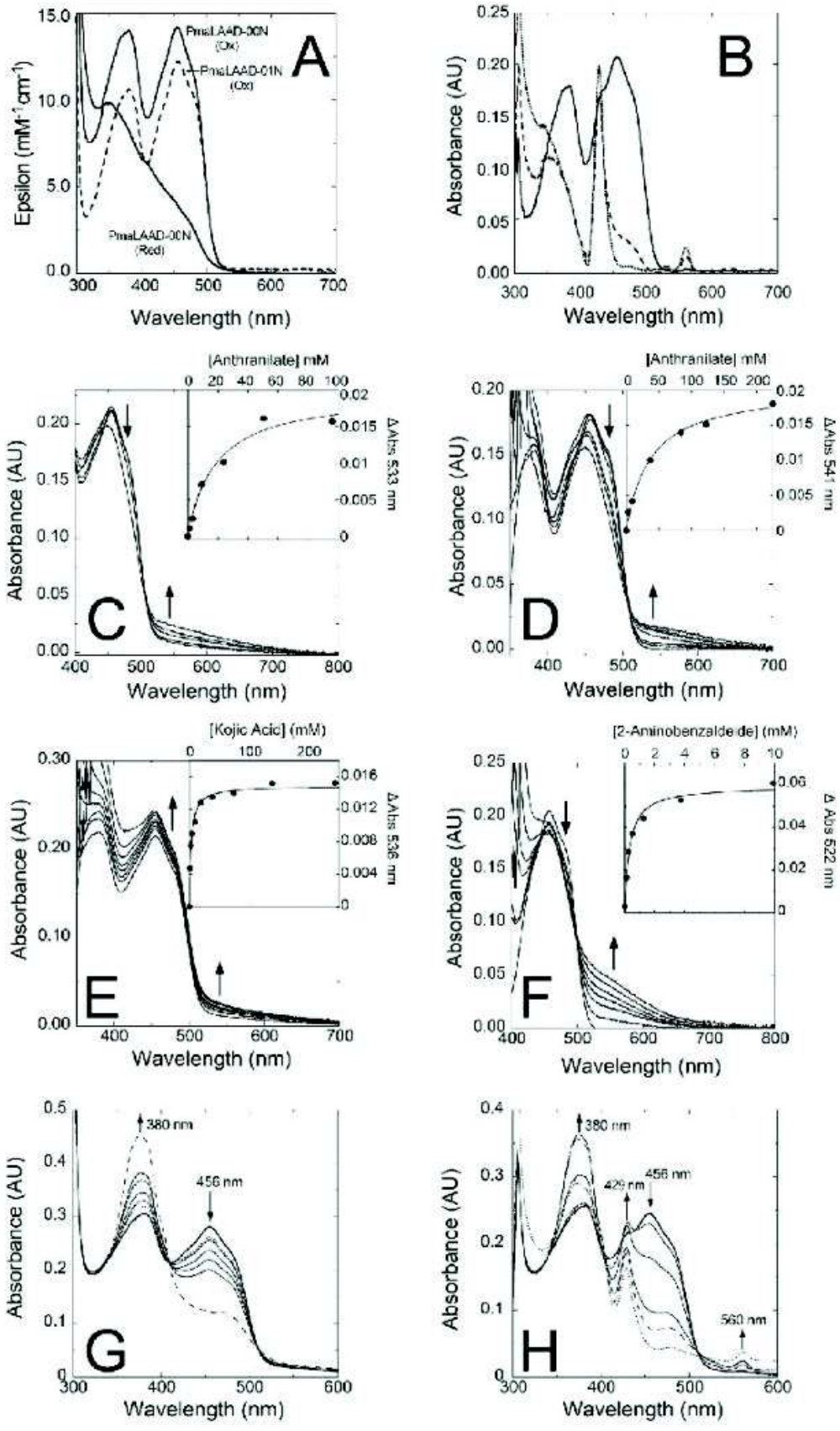
A
PmaLAAD-00N (Ox)
PmaLAAD-01N (Ox)
PmaLAAD-00N (Red)
Epsilon (mM-1cm-1)
Wavelength (nm)
B
Absorbance (AU)
Wavelength (nm)
C
[Anthranilate] mM
ΔAbs 533 nm
Absorbance (AU)
Wavelength (nm)
D
[Anthranilate] mM
ΔAbs 541 nm
Absorbance (AU)
Wavelength (nm)
E
[Kojic Acic] (mM)
ΔAbs 536 nm
Absorbance (AU)
Wavelength (nm)
F
[2-Aminobenzalde de] (mM)
Δ Abs 522 nm
Absorbance (AU)
Wavelength (nm)
G
380 nm
456 nm
Absorbance (AU)
Wavelength (nm)
H
380 nm
429 nm
456 nm
560 nm
Absorbance (AU)
Wavelength (nm)

Figure 5

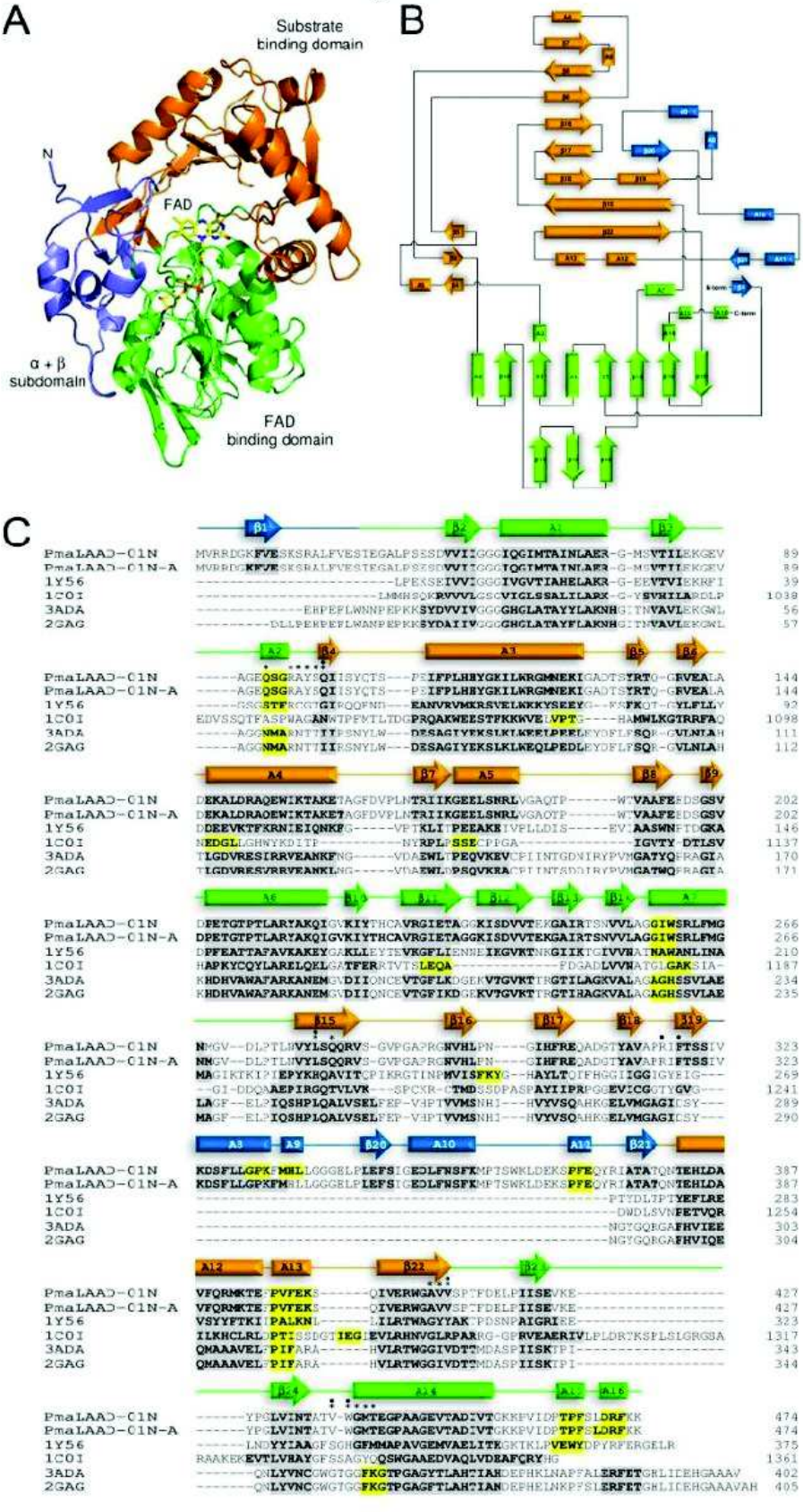
A
Substrate binding domain
N
FAD
α + β subdomain
FAD binding domain
B
C
PmaLAAO-C1N
PmaLAAO-C1N-A
1Y56
1COI
3ADA
2GAG

Figure 6

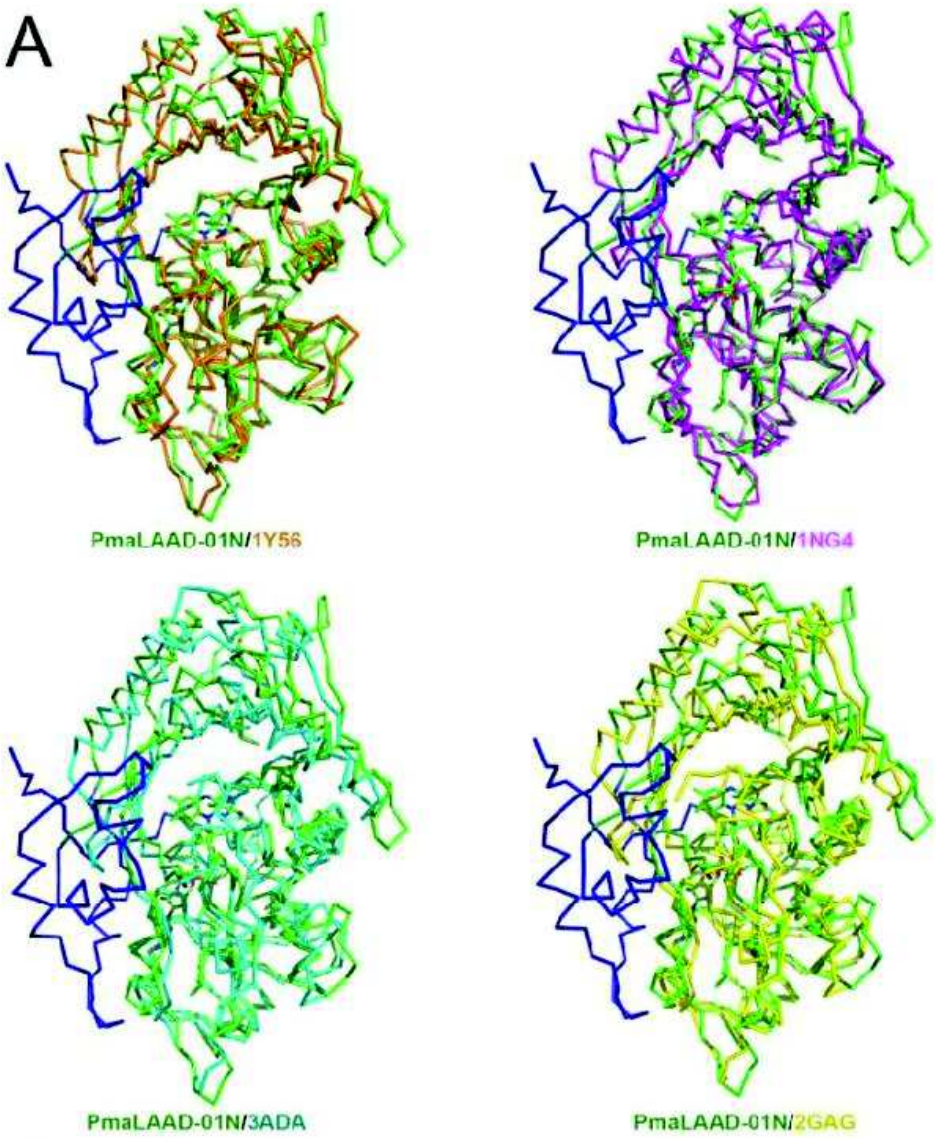
A
PmaLAAD-01N/1Y56
PmaLAAD-01N/1NG4
PmaLAAD-01N/3ADA
PmaLAAD-01N/2GAG
B
N-term
N-term
N-term
Leu52

Figure 7

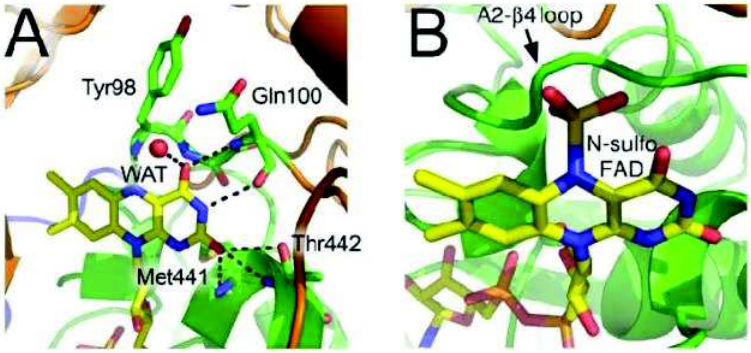

Figure 8

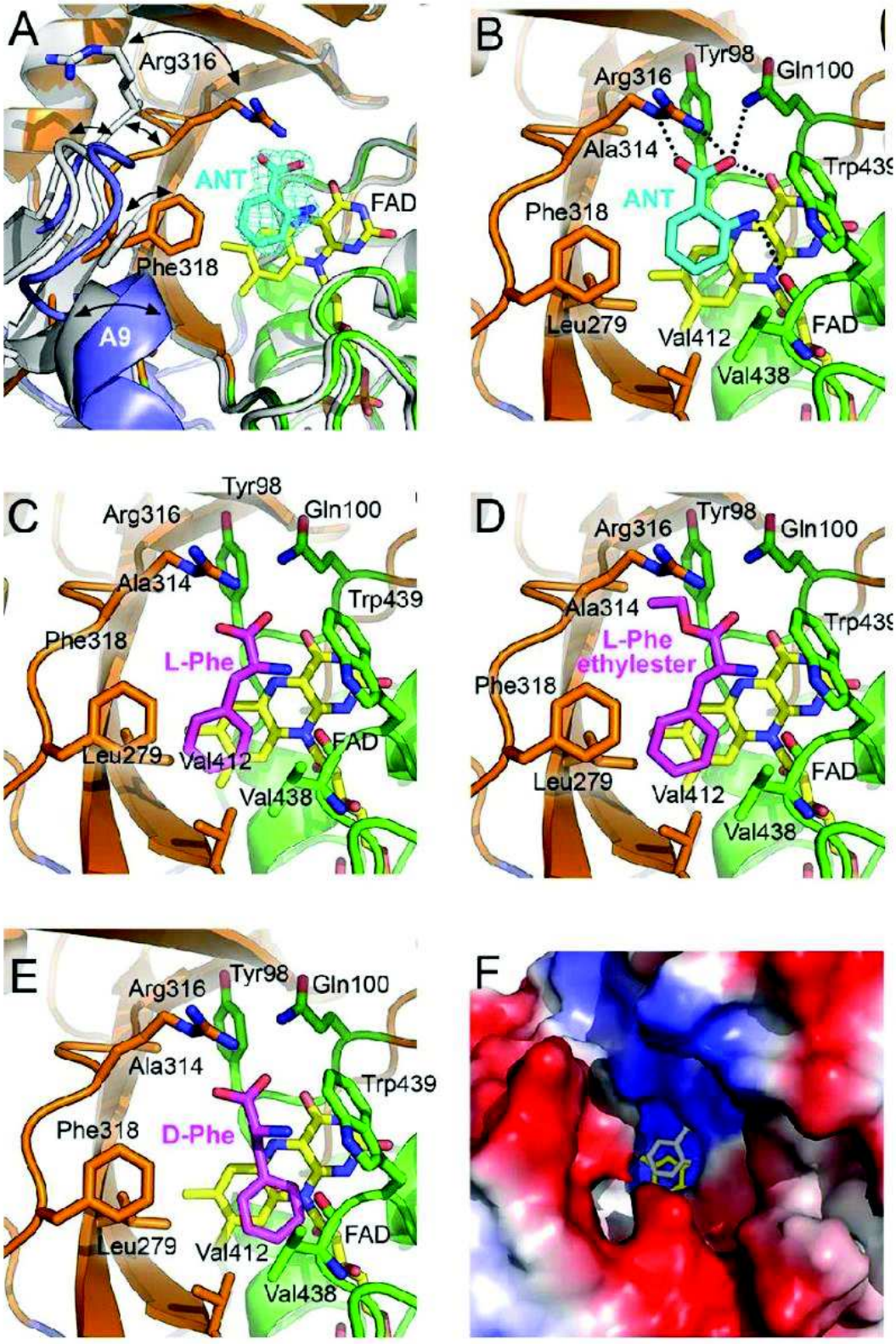
A
Arg316
ANT
FAD
Phe318
A9
B
Tyr98
Gln100
Arg316
Ala314
Trp439
ANT
Phe318
Leu279
Val412
FAD
Val438
C
Tyr98
Arg316
Gln100
Ala314
Trp439
Phe318
L-Phe
FAD
Leu279
Val412
Val438
D
Arg316
Tyr98
Gln100
Ala314
Trp439
L-Phe
ethylester
Phe318
FAD
Leu279
Val412
Val438
E
Arg316
Tyr98
Gln100
Ala314
Trp439
Phe318
D-Phe
FAD
Leu279
Val412
Val438
F

Figure 9

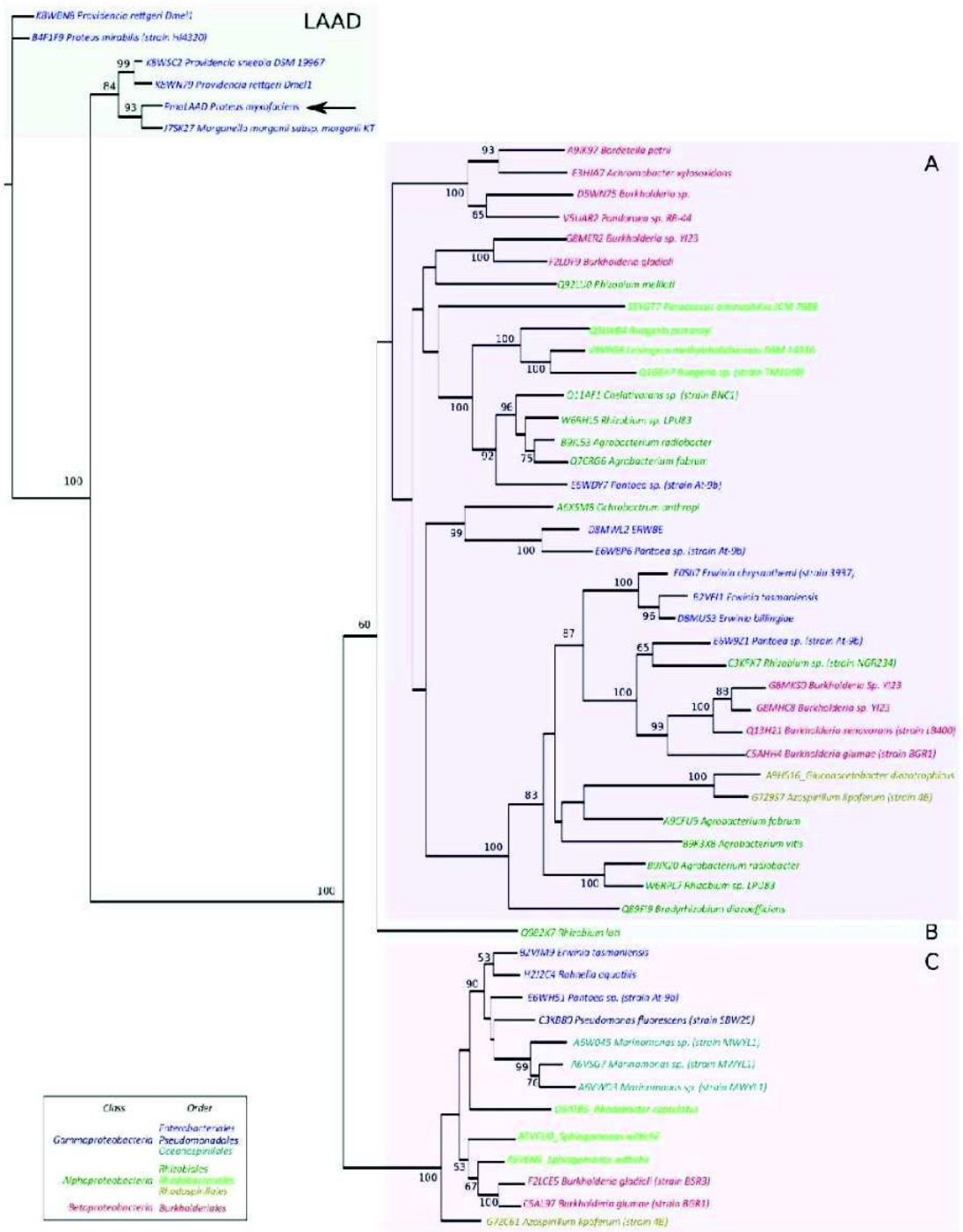
LAAD
A
B
C
Class
Order
Gammaproteobacteria
Enterobacteriales
Pseudomonadales
Oceanospirillales
Alphaproteobacteria
Rhizobiales
Rhodospirillales
Betaproteobacteria
Burkholderiales

Expression of the L-amino acid oxidase from *Rhodococcus opacus* in *Streptomyces*, a novel heterologous expression system

Abstract

L-amino acid oxidases (LAAO) are well known enzymes that catalyze the strictly enantioselective oxidation of L-amino acids to α-keto acids. The LAAO from *Rhodococcus opacus* (RoLAAO) is a broad substrate specificity enzyme that could have important applications in biocatalytic processes. These potential applications require the overproduction of the enzyme. The heterologous expression of RoLAAO was investigated in two species of the *Streptomyces* genus: *S. lividans* (strain TK24) and *S. venezuelae* (strain ATCC1055). The gene encoding for RoLAAO (AY053450) was amplified from the native source and cloned into two different expression vectors. The presence of the plasmids containing the gene coding for RoLAAO caused a significant impairment in the growth of both species. When using the constitutive expression vector pIJ86, only a very weak signal could be detected in the western blot analysis of samples from *S. lividans*. However no LAAO activity was detected in these samples. No expression of RoLAAO could be detected using the thiostrepton inducible vector pGM1190. In conclusion, the *Streptomyces* genus turned out not to be a suitable expression system for the production of L-amino acid oxidases in an amount sufficient for its biotechnological exploitation.

Introduction.

L-amino acid oxidases (LAAO) are widely distributed homodimeric flavoproteins, containing in each subunit a non-covalently bound FAD molecule as a cofactor. They catalyze the stereospecific oxidative deamination of amino acids to the corresponding α–keto acids along with the production of ammonia and hydrogen peroxide [60].

Usually LAAOs are active on a number of different L-amino acids, mainly hydrophobic ones. In particular the enzyme from the actinomicete *R. opacus* (RoLAAO) exhibits the broadest substrate specificity among known LAAOs: it is active on 39 different amino acids, mainly apolar and basic, including 17 of the proteinogenic ones. For many of its substrates it possesses a high affinity [76]. These features make it an interesting catalyst for enzymatic syntheses.

Preliminary deracemization trials have been performed on D,L-leucine and D,L-phenylalanine mixtures; after 30 minutes of reaction enantiomeric excesses of 99.2 and 99.5 %, respectively, were obtained [76]. Moreover, in batch experiments RoLAAO was able to fully convert a L-dihydroxyphenylalanine (L-DOPA) solution in 150 min [131].

In our work, we attempted the heterologous expression of the R. opacus L-AAO using a bacterial host. The development of this system will allow the introduction of mutations by site-directed mutagenesis or directed evolution to change the biochemical properties or to elucidate the reaction mechanism on a molecular level.

Experimental procedures.

Strains - *Rhodococcus opacus* strain DSM43250, has been purchased from the Deutsche Sammlung von Mikroorganismen und Zellkulturen (Braunschweig, Germany). *E. coli* strain NEB10β was purchased by New England Biolabs (Ipswich, MA, United States). *E. coli* strains ETI12567/pUZ8002, *Streptomyces lividans* strain TK24 and *Streptomyces venezuelae* strain ATCC1055 were kindly provided by the laboratory of Microbial Biotechnology of the University of Insubria (Varese, Italy).

Cloning **-** The gene encoding for LAAO was amplified by PCR from *R. opacus* colonies with the primers UP (5'-GCGCAAGCTTATGGCATTCACACGTAGATCTTTCATGAAGGGCC-3') and DN (5'-CGTGGCCCAGGAAGCCCACCACCACCATCACCACTGAAAGCTTGCGC-3') which allowed the insertion of HindIII restriction sites. The amplification was performed using the "touch down" method, in the presence of 5 % (final concentration) of DMSO.

In detail, single R. opacus colonies were picked and placed in 50 µL of 100% DMSO, vortexed briefly and stirred for 90 minutes at 100 rpm at 25 °C; 50 µL (final volume) reaction mixture was as follows: 2.5 µL cells suspension (5% final DMSO), primers 0.2 µM each, dNTPs mixture 0.2 mM each, 1X reaction buffer, 0.5 mM $MgCl_2$, 1.25 units DreamTaq DNA polymerase (Thermo Scientific).

The "touch down" PCR method requests that for the first few cycles the annealing temperature has to be lowered by 1 °C per cycle; in detail, the reaction was run as follows: 13 cycles (95 °C, 30

sec; 65 °C to 53 °C, 30 sec; 72 °C, 3 min), 5 cycles (95 °C, 30 sec; 53 °C, 30 sec; 72 °C, 2 min 15 sec), 25 cycles (95 °C, 30 sec; 62 °C, 30 sec; 72 °C, 2 min 15 sec). Agarose-gel purified PCR product and pIJ86 expression plasmid were then subject to enzymatic digestion with FastDigest HindIII restriction enzyme (Fermentas) for 30' at 37 °C and ligated using T4 phage DNA ligase (Roche) overnight at 4 °C, placing RoLAAO gene under the control of the constitutive ermEp* promoter. Correct orientation of the ligated gene was confirmed by enzymatic digestion with FastDigest BamHI and XhoI restriction enzymes (Fermentas), and the correctness of the insert was confirmed by gene sequencing.

Point mutations were corrected with QuickChange II XL site directed mutagenesis kit (Agilent), with primers G496D-for (5'-CTGCTCGAACCCGTCGACAAGATCTATTTCGCC-3') and G496D-rev (3'-GGCGAAATAGATCTTGTCGACGGGTTCGAGCAG-5'). In detail, 2 µl of ligation product were used as a template for amplification with 2.5 U of PfuUltra HF DNA polymerase (final volume 50 µl) for 18 cycles (95 °C, 50 sec; 60 °C, 50 sec; 68 °C, 8 min). The reaction product was then digested with 10 U/µl of DpnI and the reversal of the mutation was confirmed by gene sequencing.

The insert from the previous ligation was subsequently subcloned into the expression vector pGM1190; the LAAO gene and the vector were then subject to enzymatic digestion with FastDigest HindIII restriction enzyme (Fermentas) for 30' at 37 °C and ligated using T4 phage DNA ligase (Roche) overnight at 4 °C, placing RoLAAO gene under the control of the thiostrepton inducible TipA promoter. Correct orientation of the ligated gene was confirmed by

enzymatic digestion with FastDigest BamHI and XhoI restriction enzymes (Fermentas), and the correctness of the insert was confirmed by gene sequencing.

Intergeneric conjugation - Since Gram positive bacteria cannot be transformed by conventional techniques, pIJ86-RoLAAO and pGM1190-RoLAAO plasmids were inserted *Streptomyces lividans* and *venezuelae* by intergeneric conjugation mediated by *E. coli* strain ET12567/pUZ8002. In detail, both plasmids were transformed into *E. coli* strain; single colonies were inoculated in LB broth added of kanamycin (30 μg/ml), chloramphenicol (34 μg/ml) and apramycin (50 μg/ml) and grown overnight at 37 °C; afterwards they were diluted into LB added of the same antibiotics and grown at 37 °C to and OD_{600} of about 0.5 was reached. A total of 10 ml of culture was then pelleted, washed three times with 10 ml of LB without antibiotics and resuspended in 1 ml of LB without antibiotics. ≈ 10^8 *S. lividans* spores from a glycerol stock were, added of 500 μl of 2X YT broth and heat shocked for 10' at 50 °C; at the end of the heat shock 500 μl of transformed *E. coli* were mixed with 500 μl of heat shocked spores and pelleted for 3 min at 13,000 rpm at room temperature. The pellet was then resuspended in 70 μl of 2X YT, plated on two SFM + agar plates (10 μl and 60 μl, respectively) without antibiotics and incubated overnight at 30 °C. The plates were then overlaid with a solution containing 0.5 mg of apramycin to select conjugated *S. lividans* colonies and 1 mg of nalidixic acid to kill residual *E. coli* colonies, and incubated at 30 °C for a further 3 days. Single *S. lividans*

colonies were transferred onto SFM+agar plates added of apramycin (50 µg/ml) and nalidixic acid (1 mg/ml) and incubated at 30 °C for 3 days. Finally, grown colonies were transferred onto SFM+agar plates added of apramycin (50 µg/ml) and incubated at 30 °C for 3 days. The presence of the plasmid in *S. lividans* was confirmed by colony PCR.

For S. venezuelae the same procedure was adopted, except that no heat shock of the spores was necessary and the medium employed for the plates was MYM instead of SFM.

Culture conditions and protein expression **-** Wild-type RoLAAO expression was confirmed by R. opacus cultures: 500 µl of glycerol stock were inoculated in 20 ml of GYM broth (4 g/l glucose; 4 g/l yeast extract; 10 g/l malt extract) and grown overnight at 28 °C. Precultures were diluted (5 % v/v) in 100 ml of GYM and grown for a further 24 h at 28 °C, after which they were collected.

Recombinant RoLAAO was expressed in *S. lividans* in the following expression conditions: pre-precultures from 500 µL of glycerol stock were grown in 20 ml YEME or BTSB media, added with 50 µg/mL apramycin, for 96 hours at 30 °C. The pre-precultures were diluted (5 % v/v) in 50 ml of the same medium added with 50 µg/mL apramycin (preculture) and grown for a further 96 hours at 30 °C. Finally, the preculture is diluted (10 % v/v) in 100 ml of different media (BTSB, YEME, 2X YEME, V6) added with 50 µg/mL apramycin and grown for up to 240 hours. For clones harboring the pGM1190-RoLAAO plasmid, protein expression was induced

after 10 hours from the last dilution, with 5 µg/ml of thiostrepton (final concentration).

Recombinant RoLAAO was expressed in *S. venezuelae* in the same expression conditions with the exception of the last dilution, for which MYM medium instead of BTSB. For clones harboring the pGM1190-RoLAAO plasmid, protein expression was induced after 10 or 24 hours from the last dilution, with 5 µg/ml, 15 µg/ml or 50 µg/ml of thiostrepton (final concentration). Every 24 hours, after the last dilution in the case of pIJ86-RoLAAO and after thiostrepton induction in the case of pGM1190-RoLAAO, 10 ml samples of each culture were withdrawn, for the analysis of growth progression and protein expression, and divided into two 5 ml aliquots.

Growth curves - One of the two aliquots was transferred to a glass tube for setting up growth curves of each culture: in details, the aliquots were pelleted for 10' at 4000 rpm at room temperature; the pH of the supernatant was measured with pH test strips 4.5 – 10.0 (Sigma) while the residual glucose concentration with Diastix Strips (Bayer); the production of biomass was tracked by measuring the wet and dry weight (obtained after overnight incubation at 50 °C) of the pellet, and the volume of the packed mycelium (PMV), based on the graduation of the glass tube. the other aliquot was used for western blot analysis and activity assays.

Western blot analysis - For western blot analysis the 5 ml aliquots were pelleted for 10' at 4000 rpm at 4 °C; pellets were

resuspended in lysis buffer (50 mM Glycine/NaOH, pH 8.6, 10 % Glycerol, 40 µM FAD, 0.2 mg/ml PMSF) at a ratio of 5 ml per g of cells and lysed by at least 10 cycles of sonication (30 s followed by 30 s on ice). The supernatant was separated by the insoluble fraction by centrifuging for 60 min at 38,500 g at 4 °C.

Proteins in the culture broths were precipitated by treatment with tri-chloro acetic acid (TCA); in details, 1.8 ml of sample were added of 0.2 ml of 100 % (w/v) TCA (Sigma), mixed by briefly vortexing and incubated for 15 min on ice. To collect precipitated proteins the samples were centrifuged for 10 min at 38,500 g at room temperature and the supernatant was thoroughly removed. Pellets were washed by resuspending in 0.2 ml of 100 % acetone (Panreac) and centrifuged for 5 min at 38,500 g at room temperature. The supernatant was discarded and the pellets were resuspended in 0.1 ml of 1x PBS.

For activity assays, 238 mg of ammonium persulfate were added to 5 ml of culture broth and the samples were incubated under gentle stirring for 20 minutes at 4 °C followed by sitting for a further 15 minutes at 4 °C. Samples were then centrifuged at 16.000 g for 1 hour and protein pellets were resuspended in 100 µl of storage buffer (50 mM Glycine, 10% glycerol).

Protein purification - Samples were harvested by centrifugation and lysed as previously described; to attempt purification of RoLAAO from the crude extracts, 3.5 ml samples were added of NaCl to a final concentration of 1 M and loaded onto a 1 ml HiTrap chelating column; attachment of the protein was performed in

binding buffer (50 mM Glycine/NaOH, pH 8.6, 10 % Glycerol, 1 M NaCl) and elution was performed in a single step from 0 to 100 % elution buffer (50 mM Glycine/NaOH, pH 8.6, 10 % Glycerol, 0.5 M imidazole)

Enzymatic assay - Enzymatic activity on L-Ala was assayed spectrophotometrically using a 4-aminoantipyrine / HRP coupled assay. 0.9 mL of reaction mixture (10 mM L-Ala in 50 mM Glyicine/NaOH, pH 8.6, 20 µM FAD, 1.5 mM 4-aminoantipyrine, 2 mM phenol, 2.5 U of HRP) was incubated at 30 °C for 1 minute and then added of 100 µl of the protein sample. Absorbance changes were recorded at 505 nm for 5 minutes.
Enzymatic activity on L-Ala was assayed also by PAGE in non-denaturing conditions; in detail, crude extract sample were added of sample buffer without SDS and loaded onto a 7.5 % poly-acrylamide gel devoid of SDS and electrophoresis was performed at 4 °C with 1x TBE as running buffer. To allow color formation, the gel is subsequently incubated in development solution (35 mM sodium pyrophosphate, pH 8.5, 40 uM FAD, 100 mM L-Ala and 92 µg/ml INT) at 30 °C until protein bands appeared.

Results and discussion.

Wild-type RoLAAO - *R. opacus* strain DSM 43250 was grown for 24 hours at 28 °C, yielding a biomass of about 15 g of cells per liter of culture. Expression of wild-type RoLAAO was investigated by PAGE in non-denaturing conditions both in the cytoplasm of the cells, which were lysated by sonication with a yield of about 44 mg

of proteins per g of cells, and in the culture broth, which was concentrated by ultracentrifugation. RoLAAO activity was assayed on 100 mM L-Ala as a substrate, and after 3 hours of incubation at 30 °C the appearance of a specific band could be observed in the cytosolic sample, while no signal could be detected in the culture broth even after overnight incubation. We thus confirmed the intracellular expression of RoLAAO despite the presence of the putative secretion signal peptide (Fig. 1).

Enzymatic activity in the crude extract was quantified by a 4-aminoantipyrine/HRP coupled assay on 10 mM L-Ala as a substrate: an activity of about 0.2 U/ml was measured, corresponding to a specific activity of about 24 mU per mg of protein, in good agreement with data in literature (32 mU/mg; Geueke and Hummel, 2002).

Recombinant RoLAAO - To achieve overexpression of recombinant RoLAAO, two species of Streptomyces genus were employed: *S. lividans* which lacks a system of endogenous endonucleases and should therefore be easier to conjugate, and *S. venezuelae*, which should display a faster growth rate. Recombinant clones were obtained by intergeneric conjugation from *E. coli* strain ET12567/pUZ8002. We obtained 36 pIJ86-RoLAAO and 20 pGM1190-RoLAAO *S. lividans* recombinant clones; when *S. venezuelae* was employed, we obtained 8 pIJ86-RoLAAO and 20 pGM1190-RoLAAO clones (Table 1).

Streptomyces lividans and *venezuelae* consume glucose with a similar rate, causing its depletion in about 48 hours. For the rest

the growth of the two microorganisms show marked differences: S. lividans grows at a much faster rate compared to S. venezuelae, as they reach a biomass of 104 grams of mycelium per liter of culture after 96 hours after the last dilution, and of 52 grams of mycelium per liter of culture after 240 hours after the last dilution, respectively (Fig. 2).

An important aspect that should be pointed out though, is the lack of reproducibility in the growth trials: in fact only using *S. lividans* and only in the case reported above, a good growth curve could be obtained.

Concerning *S. lividans*, the control cultures with the wild-type organism show much better growth parameters than the recombinant clones; this could be due to the synthesis of a very small quantity of RoLAAO, which, although below our detection limit, could be sufficient to produce an amount of H_2O_2 that is toxic for the cells; or the presence of the plasmid itself could cause a significant metabolic burden to the cells. The latter hypothesis seems the most plausible, since the effect on the growth has been observed in all clones harboring both pIJ86 and pGM1190 plasmids, independent of the presence of the gene, or of the inducer.

In the case of *S. venezuelae* no optimal conditions could be obtained, in all cases the growth was fragmented, if not completely absent, for both the wild-type and conjugated clones (Fig. 3).

In one case, western blot analysis of a S. lividans clone harboring pIJ86-RoLAAO plasmid showed the presence of a faint band at the expected molecular weight in the crude extracts of the aliquots

withdrawn after 48 h and 72 h; this samples were loaded onto a HiTrap Chelating column to attempt purification of RoLAAO. A single peak was eluted with 0.5 M imidazole, but following SDS-PAGE and western blot analysis the presence of the protein in the fraction could not be confirmed; moreover, when a 4-aminoantipyrine / HRP coupled assay was employed, no L-amino acid oxidase activity on L-Ala as a substrate could be detected.

A band at the expected molecular weight was observed also in the culture broths of all the aliquots withdrawn after the final dilution except T_0. In spite of this, following concentration of the protein samples and 4-aminoantipyrine / HRP coupled assay, no L-amino acid oxidase activity on L-Ala as a substrate could be detected (Fig. 4).

Protein expression in *S. lividans* clones harboring pGM1190-RoLAAO plasmid was induced with 5 μg/ml (final concentration) of thiostrepton, 10 hours after the last dilution; following SDS-PAGE analysis, in all cases no expression of RoLAAO could be detected.

S. venezuelae clones harboring pIJ86-RoLAAO plasmid showed no expression of the protein under any condition. Protein expression in clones harboring pGM1190-RoLAAO plasmid was induced with 5 μg/ml, 15 or 50 μg/ml, (final concentration) of thiostrepton, 10 or 24 hours after the last dilution but following SDS-PAGE analysis, in all cases no expression of RoLAAO could be detected.

In conclusion, while allowing to circumvent the problem of the formation of inclusion bodies, the slow and problematic growth in the presence of exogenous plasmids coupled to the very low

expression yields make the genus Streptomyces an unsuitable alternative to *E. coli* for the heterologous expression of microbial L-amino acid oxidases.

Figures and tables

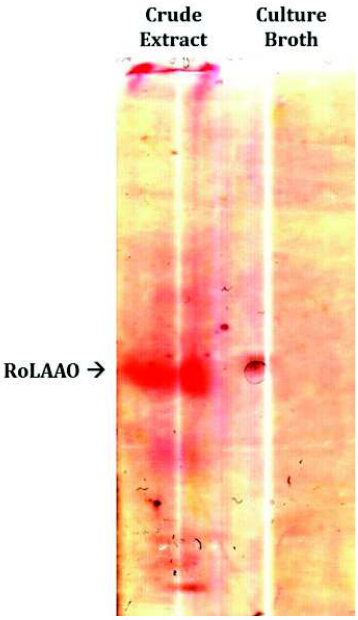

Figure 1. Native PAGE of R. opacus samples. 30 µl samples were loaded onto a 7.5 % polyacrylamide gel and run at 4 °C. The gel was subsequently incubated in the development solution containing 100 mM L-Ala and 92 µg/ml INT, until the appearance of the band

Table 1. Number of Streptomyces clones obtained by intergeneric conjugation

Species	Plasmid	Clones obtained	Checked by colony PCR	Positives
S. lividans	pIJ86-RoLAAO	36	5	5
	pGM1190-RoLAAO	20	6	5
S. venezuelae	pIJ86-RoLAAO	8	5	2
	pGM1190-RoLAAO	20	6	6

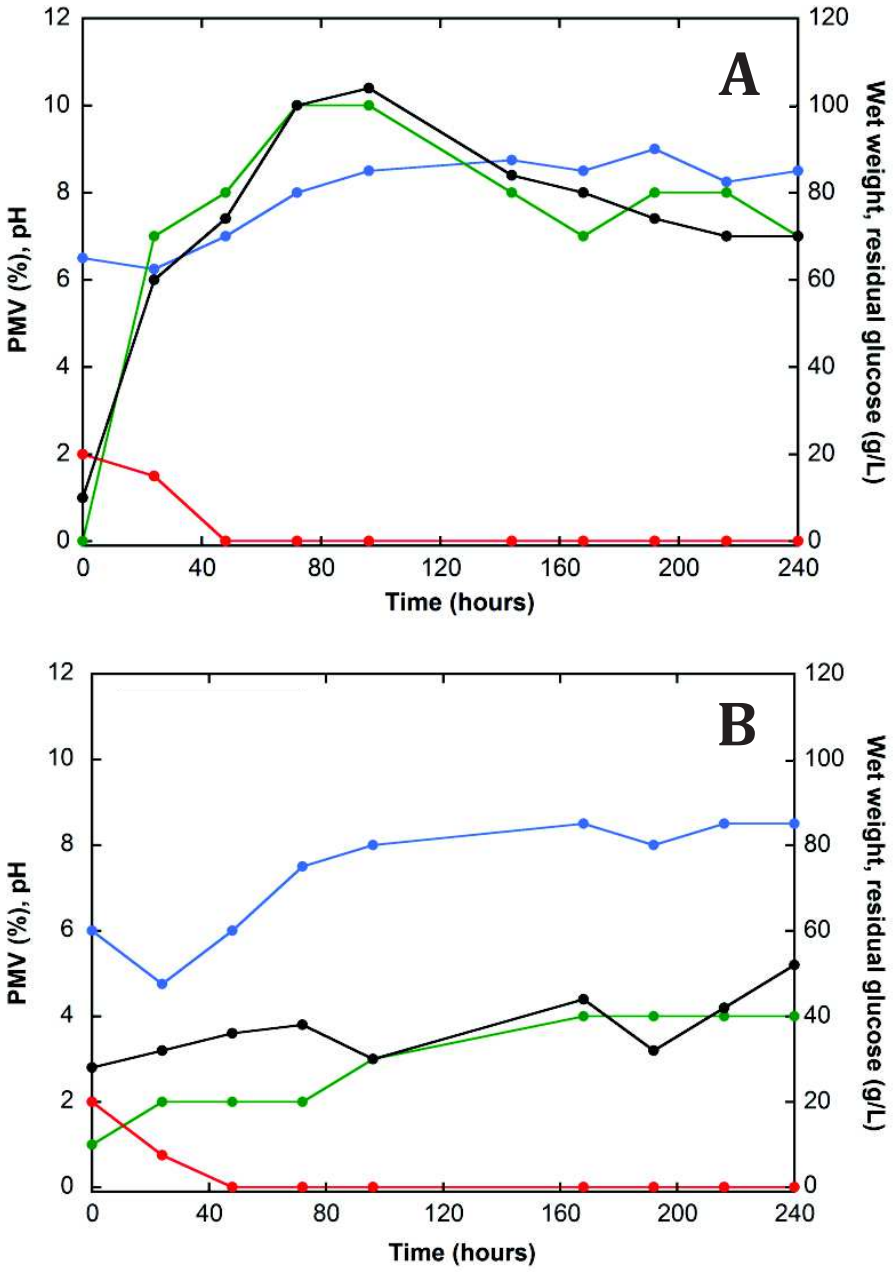

Figure 2. Growth curves of A) *Streptomyces lividans* clone 31 and B) *Streptomyces venezuelae* clone 5. Red = residual glucose (g/L). Black = wet weight (g/L). Blue = pH. Green = PMV (%)

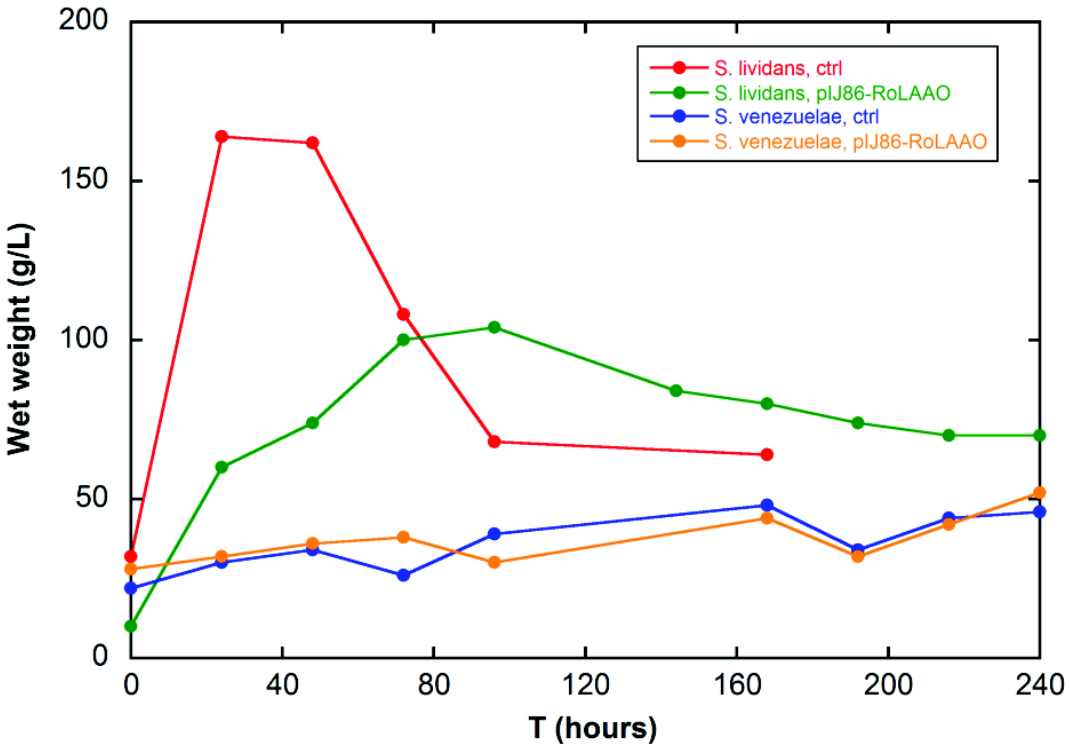

Figure 3. Comparison of the rate of growth of different *Streptomyces* clones. Red = control *S. lividans* strain. Green = pIJ86-RoLAAO harboring *S. lividans* strain. Blue = *S. venezuelae* control strain. Orange = pIJ86-RoLAAO harboring *S. venezuelae* strain.

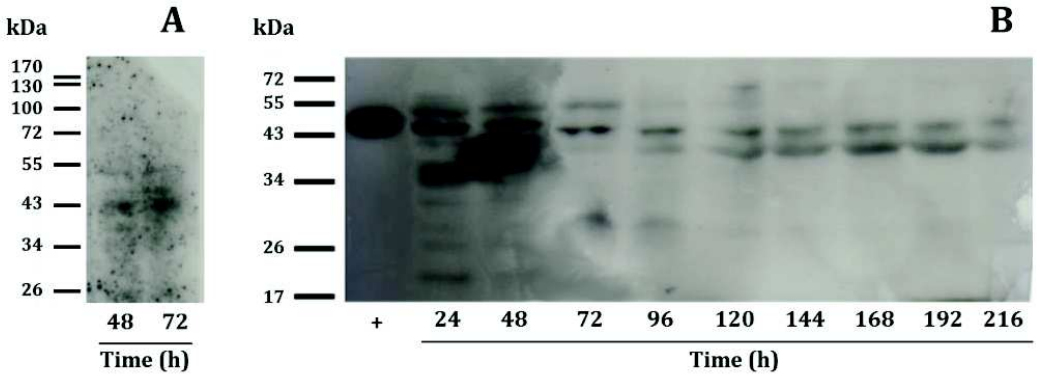

Figure 4. Western blot analysis of *Streptomyces lividans* samples. In both cases a His Probe antibody was used. Exposure time = 30 min. A) Crude extract samples. B) Culture broth samples. + = RoLAAO from *E. coli* inclusion bodies.

Discussion

It is now commonly accepted that the great molecular biodiversity of contemporary enzymes has stemmed from their divergent evolution from ancestral progenitors, a phenomenon in which enzyme promiscuity has played a key role.

Enzyme promiscuity is defined as the presence of auxiliary enzyme activities, in addition to the one for which an enzyme has evolved, that are not part of the organism physiology [2]. This ability of enzymes to catalyze potentially advantageous functions grants the organism the necessary adaptability to face variations of its environment, thus enhancing the probability of survival and reproduction [132].

A well-known example of enzymatic promiscuity is represented by the enzymes belonging to the family of flavoproteins, which have evolved to perform a wide variety of enzymatic reactions in Nature [28]. A paradigmatic example of the capacity of flavoproteins to acquire new functions is represented by members of the amino acid oxidase group, which have evolved to catalyze an extremely wide range of reactions, depending on the organism (or tissue) in which they are expressed [44, 60, 65]. This ability, along with their remarkable enantioselectivity, makes these enzymes an ideal scaffold for the *in vitro* evolution of novel catalytic activities to perform a wide range of biotransformations, such as the resolution of racemic mixtures of amino acids. The exploitation of D-amino acid oxidases for this purpose is already a well-established procedure [43], while the use of LAAOs for the same aim is still hampered by the difficulty of their heterologous expression. In fact, the most studied members of this class are the enzymes

purified from the snake venom, which are extensively glycosylated, and thus cannot be expressed in an active form and at high levels as recombinant proteins in a prokaryotic expression system.

This PhD project has been focused on the identification of novel microbial L-amino acid oxidases with the aim to define their structure/function relationships and understand the evolutionary mechanisms that led to their great diversification and specialization, related to their specific physiological role.
The information obtained in this work will be also useful for the successive modification of the biochemical properties of these flavoproteins for their employment in biocatalytic processes.

The first enzyme that was investigated was the aminoacetone oxidase from the microorganism of the oral-cavity S*treptococcus oligofermentans* (SoAAO). We demonstrated that, differently from what previously reported, SoAAO is not a "canonical" LAAO: this flavoprotein is not able to stabilize any semiquinone species of FAD, it does not react with sodium sulfite and its midpoint redox potential (-324 mV) is unusually low in comparison to the one of other flavooxidases. From a functional point of view, SoAAO shows a low but significant activity (about 0.05 U/mg of protein) on aminoacetone (its preferred substrate), while it has only a very low promiscuous activity on different L-amino acids. The solution of the three-dimensional structure of SoAAO confirmed that this protein does not belong to the group of L-amino acid oxidases: in

fact, SoAAO is a monomeric enzyme formed by three domains and represents a paradigm for a novel class of bacterial flavoproteins. The inspection of the 3D structure of SoAAO in complex with the substrate analog O-methyl glycine, revealed that the enzyme could catalyze the condensation of two aminoacetone molecules to yield 2,5-dimethylpyrazine, as confirmed also by mass spectrometry analysis. We thus propose that, in *S. oligofermentans*, this compound is the actual product of aminoacetone degradation and not methylglyoxal as previously suggested [84]. Accordingly, in this microorganism SoAAO could act as a scavenger of aminoacetone (a prooxidant molecule) thus protecting the cell from a ROS-mediated oxidative damage. Its low specific activity could be a consequence of the low intracellular levels of aminoacetone (about 5.5 ng per mg of cells) [84].

The second enzyme that was investigated is the L-amino acid deaminase from *Proteus myxofaciens* (PmaLAAD). Unlike SoAAO, PmaLAAD is active on several L-amino acids, with a substrate specificity that overlaps the one of other canonical LAAOs, both microbial (e.g., LAAO from *R. opacus*) or eukaryotic (e.g., LAAO from *C. rhodostoma*). Its three-dimensional structure was solved at a 1.7 Å resolution, both in the free enzyme and in complex with the competitive inhibitor anthranilate; it was similar to the one of canonical flavooxidases. Nonetheless two main features distinguish PmaLAAD from classical LAAOs: first, this flavoenzyme is a type II membrane bound protein, with its catalytic site facing the periplasmic side of the bacterial membrane, and, second, it

does not use molecular oxygen as a direct electron acceptor (i.e. it does not produce H_2O_2). Instead, we demonstrated that the activity of PmaLAAD results into the reduction of a membrane-associated cytochrome b, suggesting a possible electron flow from PmaLAAD to this membrane protein. Indeed, b-type cytochromes usually interact with flavin containing oxidoreductases forming large membrane complexes, such as, for example, the respiratory complex I [133]. In the case of membrane-bound flavoprotein Hydrogenase 1 from *E. coli*, a transfer of electrons to a cytochrome b mediated by four iron-sulphur centers of the flavoprotein was demonstrated [134]. However we cannot exclude that *in vivo* transfer of electrons from the flavin of PmaLAAD to the heme of cytochrome b could be mediated by a non-proteic partner, such as ubiquinone (as proposed for *P. mirabilis* in [37] and [59]). In any case, the proposed final electron acceptor of this reaction chain is a cytochrome oxidase, which would, in turn, reduce molecular oxygen through a one-electron transfer [37]. This could explain the need for O_2 in order for PmaLAAD to be fully active. PmaLAAD is an example of the ability of some flavoproteins to accept two electrons from the substrate and transfer them one by one to a suitable membrane acceptor. We propose that PmaLAAD is involved in catabolic utilization of free exogenous L-amino acids: it catalyzes their oxidative deamination, and transfers the reducing equivalents to the electron-transfer chain of *Proteus* membrane.

In conclusion, our research allowed us to identify and characterize two novel flavoproteins which, from a biochemical point of view,

are quite different from one another. As an example, concerning the catalyzed reaction, SoAAO is able to directly reduce molecular oxygen by a two electron transfer with the concomitant production of H_2O_2, while PmaLAAD uses cytochrome b as electron acceptor.

Enantiomeric amino acids oxidases have evolved a three points system to bind their substrates. The αCOOH of the amino acid binds to an arginine residue via a salt bridge and is further stabilized by a hydrogen bond with a tyrosine residue (e.g., Arg90 and Tyr372 in CrLAAO or Arg285 and Tyr223 in DAAO from *R. gracilis*), while the αNH_2 group is usually hydrogen bonded with the main chain carbonyl of a small residue (e.g., Gly464 in CrLAAO or Ser335 in RgDAAO). The substrate specificity is determined by the side chains of the residues, positioned above the isoalloxazine ring, which interact with side chain of the substrate.

The architecture of the active site of PmaLAAD reveals a common evolutionary origin with canonical LAAOs. In the three-dimensional structure of the complex with anthranilate, the αCOOH of the inhibitor molecule is hydrogen bonded with Arg316 and Gln100 (as it happens in RoLAAO with Gln228). Interestingly, if we consider the aminoacidic sequence, during evolution these two residues switched their positions, but the spatial disposition of their side chains and their interactions with the αCOOH of the substrate were preserved: Gln100 occupies the position of Arg90 of CrLAAO, while the Arg316 of PmaLAAD overlaps the tyrosine residue at position 372. Moreover, in analogy with other LAAOs, the NH_2 of anthranilate is stabilized by a main chain carbonyl of

the protein. Concerning substrate specificity, the specific residues which interact with the side chain of the substrate acid are not conserved (with the exception of a tryptophan on the side of the pyrimidine moiety - Trp439 in PmaLAAD, Trp467 in RoLAAO, and Trp465 in CrLAAO), but the hydrophobicity of the specificity pocket is retained (Fig. 14).

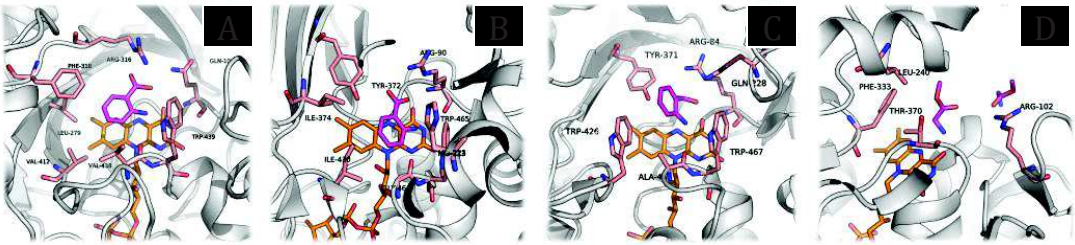

Figure 14. Detail of the active site cavity of A) PmaLAAD. B) CrLAAO. C) RoLAAO. D) SoAAO. All the structures were resolved in complex of the substrate analog anthranilate (A, B, C) od O-methyl glycine (D). Protein backbone is shown as gray ribbons. FAD cofactor (orange), ligand (purple) and the side chains of relevant residues of the protein (pink) are shown as sticks

Comparison of the structure of PmaLAAD in the free form and in complex with anthranilate showed that Arg316 undergoes a drastic conformational change upon the binding of the ligand, causing the insertion of its side chain into the active site cavity. Similarly, the microbial flavoprotein RgDAAO also possesses a residue which shifts its conformation following ligand binding, namely Tyr238 [135]. We propose that this conformational change could favor the binding (by electrostatic interactions) and correct positioning (in a catalytically competent orientation) at the active site. In addition, the flexibility of Arg316 could provide a broad substrate specificity by fine-tuning the substrate binding mode according to the size of its side chain. These features could increase the efficiency of PmaLAAD to oxidize different type of

AAs, granting its native organism the ability to grow on L-amino acids as the main carbon and nitrogen sources.

The active site entrance of different LAAOs is quite different. In RoLAAO the active site is a cleft of the surface of the protein, and its entrance is very large. Similarly, the active site of PmaLAAD is a quite broad cavity, although its entrance is partially delimited by the additional α/β subdomain. In eukaryotic LAAOs the active site is further less accessible; in fact, in these proteins the active site entrance is a narrow funnel formed by an additional α-helical domain. Interestingly, superimposition of the 3D structure of PmaLAAD and CrLAAO, shows that this domain is placed in a position that almost completely closes the access to the active site of PmaLAAD. It is thus tempting to propose a potential evolutionary route from prokaryotic to eukaryotic LAAOs, in which the shift from a general metabolic function to a more specific role has been achieved by the (subsequential?) implementation of additional domains.

The higher accessibility of the FAD cofactor of PmaLAAD (which is quite exposed to the solvent) might be explained by the necessity of PmaLAAD to directly interact with cytochrome b.

A direct comparison between the structures of SoAAO and canonical LAAOs cannot be performed, due to their highly different general and active site architecture. In the case of SoAAO, the arginine residue which should bind the carboxyl group of the substrate is present in the active site region (Arg102), but it is shifted outwards of about 5 Å, thus preventing the binding of L-amino acids in a catalytically competent way. Instead, Arg102 is

proposed to be involved (with Arg49) in the orientation of a second aminoacetone molecule to favor the condensation reaction. Furthermore, in SoAAO the active site cavity is very small: in fact, large part of the space above the isoalloxazine, which should be occupied by the substrate side chain, is occupied by Phe333. These features explain the almost absent activity of SoAAO on L-amino acids. It is plausible that the ancestor of SoAAO could be a canonical LAAO in which the aminoacetone oxidase activity represented a promiscuous activity. During evolution, the introduction of few mutations dramatically decreased the LAAO activity and, at the same time, slightly enhanced the reactivity on aminoacetone, possibly in response to the "appearance" of this toxic compound in the metabolome of the cells. Given the wide structural differences of SoAAO, we expect that this divergence event has happened very early in the evolution of LAAOs.

Interestingly, the recruitment of novel domains by both SoAAO and PmaLAAD could represent the necessity of these proteins to interact with other protein partner(s), namely some putative aminoacetone "sensor" or a cytochrome b, respectively. Thus these proteins represent also an example of molecular evolution by the addition (e.g., through gene shuffling) of new existing domains to a "Rossman fold" scaffold (i.e. modular evolution). A significant degree of similarity between SoAAO and PmaLAAD is observed only in the regions involved in the FAD binding (in fact both belong to the GR2 subfamily of flavoproteins), while no sequence conservation is apparent in other parts of the protein (Fig. 15). Similarly, a very low degree of identity is observed with eukaryotic

LAAOs (e.g., from snake venom or unicellular algae). Also in this case, the only conserved region is represented by the FAD binding domain, thus providing further evidence for the hypothesis of the addition of existing domains to a Rossman fold scaffold [136].

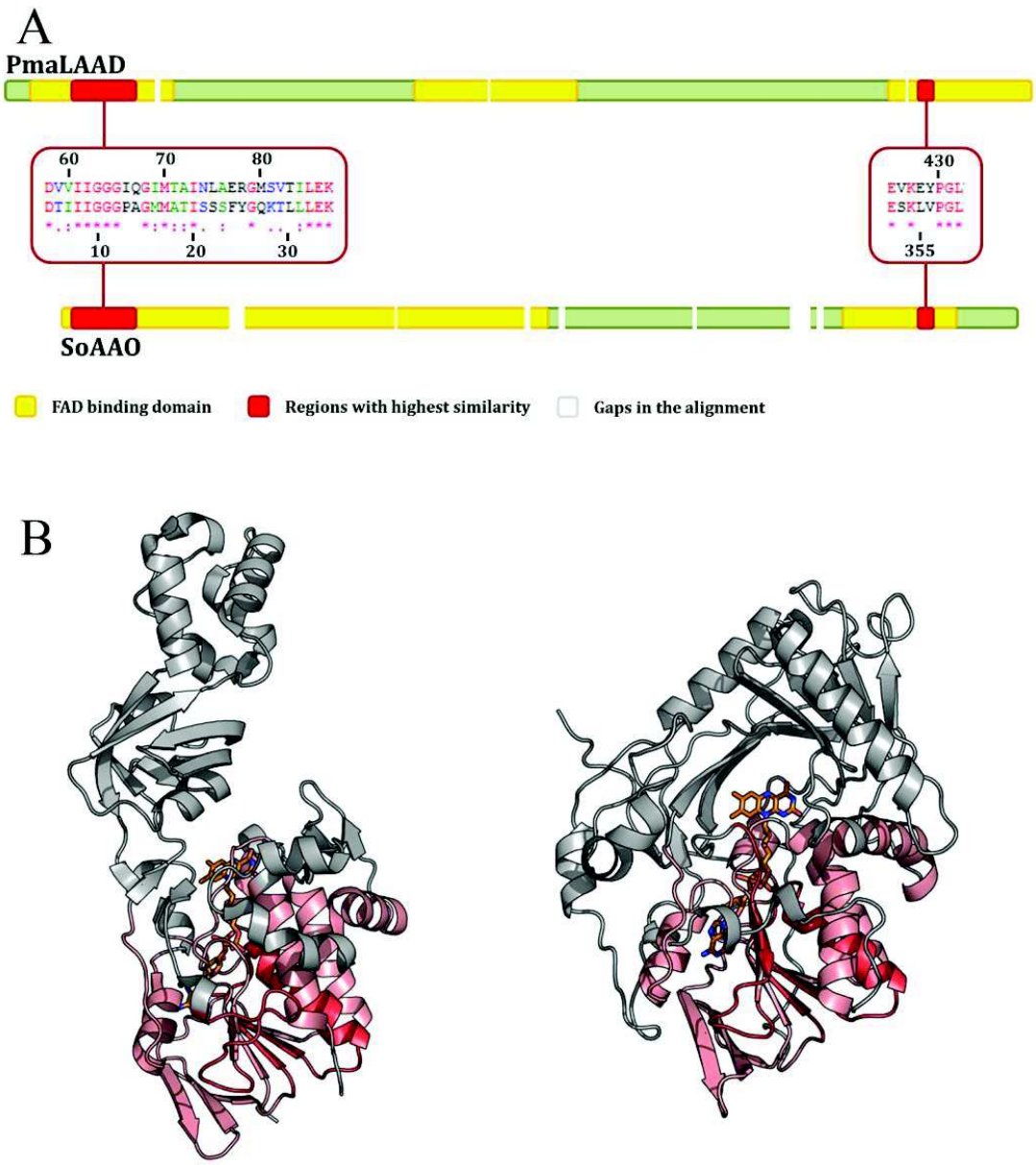

Figure 15. Comparison of PmaLAAD and SoAAO. A) Sequence alignment between PmaLAAD and SoAAO. The FAD binding domain is shown in yellow. The regions with the highest degree of similarity are highlighted in red and the alignment is shown. Gaps in the alignment are shown as white interruptions. B) Ribbon representation of SoAAO and PmaLAAD. In red are the regions with the highest degree of similarity in the alignment. In pink are the overlapping regions of the two proteins with a lower degree of similarity. The FAD cofactor is shown in stick representation.

The Rossman fold motif, like other nucleotide binding motifs such as the P-loop [137], is present in a very high number of functionally unrelated proteins. Both of these motifs are involved in the binding of the phosphate backbone of mono and dinucleotides [138].

Thus, it can be proposed that the putative *last universal common ancestor* of all flavoproteins was a small peptide possessing a Rossman fold-like structure, with the ability to bind nucleotides, which diverged from other nucleotide binding peptides in the early stages of the evolution of proteins, and that originated, by divergent evolution, the impressive structural, functional and biological diversity of the members of this enzymatic family we see today.

REFERENCES

[1] Jensen, R.A., *Enzyme recruitment in evolution of new function*. Annu Rev Microbiol, 1976. 30: p. 409-25.

[2] Khersonsky, O., and Tawfik, D.S., *Enzyme promiscuity: a mechanistic and evolutionary perspective*. Annu Rev Biochem, 2010. 79: p. 471-505.

[3] Hult, K., and Berglund, P., *Enzyme promiscuity: mechanism and applications*. Trends Biotechnol, 2007. 25(5): p. 231-8.

[4] James, L.C., and Tawfik, D.S., *Conformational diversity and protein evolution--a 60-year-old hypothesis revisited*. Trends Biochem Sci, 2003. 28(7): p. 361-8.

[5] Aharoni, A., Gaidukov, L., Khersonsky, O., McQ Gould, S., Roodveldt, C., and Tawfik, D.S., *The 'evolvability' of promiscuous protein functions*. Nat Genet, 2005. 37(1): p. 73-6.

[6] Roodveldt, C., and Tawfik, D.S., *Shared promiscuous activities and evolutionary features in various members of the amidohydrolase superfamily*. Biochemistry, 2005. 44(38): p. 12728-36.

[7] Michaud, G.A., Salcius, M., Zhou, F., Bangham, R., Bonin, J., Guo, H., Snyder, M., Predki, P.F., and Schweitzer, B.I., *Analyzing antibody specificity with whole proteome microarrays*. Nat Biotechnol, 2003. 21(12): p. 1509-12.

[8] James, L.C., and Tawfik, D.S., *The specificity of cross-reactivity: promiscuous antibody binding involves specific hydrogen bonds rather than nonspecific hydrophobic stickiness*. Protein Sci, 2003. 12(10): p. 2183-93.

[9] Lancet, D., Sadovsky, E., and Seidemann, E., *Probability model for molecular recognition in biological receptor repertoires: significance to the olfactory system*. Proc Natl Acad Sci U S A, 1993. 90(8): p. 3715-9.

[10] Chen, K., and Arnold, F.H., *Tuning the activity of an enzyme for unusual environments: sequential random mutagenesis of subtilisin E for catalysis in dimethylformamide*. Proc Natl Acad Sci U S A, 1993. 90(12): p. 5618-22.

[11] Wang, S.C., Johnson, W.H., and Whitman, C.P., *The 4-oxalocrotonate tautomerase- and YwhB-catalyzed hydration of 3E-haloacrylates: implications for the evolution of new enzymatic activities*. J Am Chem Soc, 2003. 125(47): p. 14282-3.

[12] Catrina, I., O'Brien, P.J., Purcell, J., Nikolic-Hughes, I., Zalatan, J.G., Hengge, A.C., and Herschlag, D., *Probing the origin of the compromised catalysis of E. coli alkaline phosphatase in its promiscuous sulfatase reaction*. J Am Chem Soc, 2007. 129(17): p. 5760-5.

[13] Fernández-Gacio, A., Codina, A., Fastrez, J., Riant, O., and Soumillion, P., *Transforming carbonic anhydrase into epoxide synthase by metal exchange*. Chembiochem, 2006. 7(7): p. 1013-6.

[14] Jin, W., Yu, Z., He, W., Ye, W., and Xiao, W.J., *Efficient Rh(I)-catalyzed direct arylation and alkenylation of arene C-H bonds via decarbonylation of benzoic and cinnamic anhydrides*. Org Lett, 2009. 11(6): p. 1317-20.
[15] Kazlauskas, R.J., *Enhancing catalytic promiscuity for biocatalysis*. Curr Opin Chem Biol, 2005. 9(2): p. 195-201.
[16] Jao, S.C., Huang, L.F., Tao, Y.S., and Li, W.S., *Hydrolysis of organophosphate triesters by Escherichia coli aminopeptidase P*. J Mol Catal B Enzym, 2004. 27: p. 7-12.
[17] O'Brien, P.J., and Herschlag, D., *Catalytic promiscuity and the evolution of new enzymatic activities*. Chem Biol, 1999. 6(4): p. R91-R105.
[18] Draganov, D.I., Teiber, J.F., Speelman, A., Osawa, Y., Sunahara, R., and La Du, B.N., *Human paraoxonases (PON1, PON2, and PON3) are lactonases with overlapping and distinct substrate specificities*. J Lipid Res, 2005. 46(6): p. 1239-47.
[19] Lu, X., Li, L., Wu, R., Feng, X., Li, Z., Yang, H., Wang, C., Guo, H., Galkin, A., Herzberg, O., Mariano, P.S., Martin, B.M., and Dunaway-Mariano, D., *Kinetic analysis of Pseudomonas aeruginosa arginine deiminase mutants and alternate substrates provides insight into structural determinants of function*. Biochemistry, 2006. 45(4): p. 1162-72.
[20] Rothman, S.C., and Kirsch, J.F., *How does an enzyme evolved in vitro compare to naturally occurring homologs possessing the targeted function? Tyrosine aminotransferase from aspartate aminotransferase*. J Mol Biol, 2003. 327(3): p. 593-608.
[21] Babtie, A., Tokuriki, N., and Hollfelder, F., *What makes an enzyme promiscuous?* Curr Opin Chem Biol, 2010. 14(2): p. 200-7.
[22] Ohno, S., *Evolution by Gene Duplication*. London-New York: Allen & Unwin/Springer-Verlag, 1970. 160 pp.
[23] Bershtein, S., Segal, M., Bekerman, R., Tokuriki, N., and Tawfik, D.S., *Robustness-epistasis link shapes the fitness landscape of a randomly drifting protein*. Nature, 2006. 444(7121): p. 929-32.
[24] Varadarajan, N., Gam, J., Olsen, M.J., Georgiou, G., and Iverson, B.L., *Engineering of protease variants exhibiting high catalytic activity and exquisite substrate selectivity*. Proc Natl Acad Sci U S A, 2005. 102(19): p. 6855-60.
[25] Khersonsky, O., Roodveldt, C., and Tawfik, D.S., *Enzyme promiscuity: evolutionary and mechanistic aspects*. Curr Opin Chem Biol, 2006. 10(5): p. 498-508.
[26] O'Loughlin, T.L., Green, D.N., and Matsumura, I., *Diversification and Specialization of HIV Protease Function During In Vitro Evolution*. Mol Biol Evol, 2006. 23(4): p. 764-72.
[27] Trifonov, E.N., and Frenkel, Z.M., *Evolution of protein modularity*. Curr Opin Struct Biol, 2009. 19(3): p. 335-40.
[28] Ghisla, S., and Massey, V., *Mechanisms of flavoprotein-catalyzed reactions*. Eur J Biochem, 1989. 181(1): p. 1-17.
[29] Gibson, Q.H., Massey, V., and Atherton, N.M., *The nature of compounds present in mixtures of oxidized and reduced flavin mononucleotides*. Biochem J, 1962. 85: p. 369-83.

[30] Swinehart, J.H., *Electron transfer in the flavin mononucleotide system*. J Am Chem Soc, 1966. 88(5): p. 1056-8.
[31] Ehrenberg, A., Müller, F., and Hemmerich P., *Basicity, visible spectra, and electron spin resonance of flavosemiquinone anions*. Eur J Biochem, 1967. 2(3): p.286-93.
[32] Massey, V., and Hemmerich, P., *Active-site probes of flavoproteins*. Biochem Soc Trans, 1980. 8(3): p. 246-57.
[33] Massey, V., Strickland, S., Mayhew, S.G., Howell, L.G., Engel, P.C., Matthews, R.G., Schuman, M., and Sullivan, P.A., *The production of superoxide anion radicals in the reaction of reduced flavins and flavoproteins with molecular oxygen*. Biochem Biophys Res Commun, 1969. 36(6): p. 891-7.
[34] Spector, T., and Massey, V., *p-Hydroxybenzoate hydroxylase from Pseudomonas fluorescens. Evidence for an oxygenated flavin intermediate*. J Biol Chem, 1972. 247(17): p. 5632-6.
[35] Strickland, S., and Massey, V., *The mechanism of action of the flavoprotein melilotate hydroxylase*. J Biol Chem, 1973. 248(8): p. 2953-62.
[36] Entsch, B., Ballou, D.P., and Massey, V., *Flavin-oxygen derivatives involved in hydroxylation by p-hydroxybenzoate hydroxylase*. J Biol Chem, 1976. 251(9): p. 2550-63.
[37] Van Wielink, J.E., Reijnders, W.N., Oltmann, L.F., and Stouthamer, A.H., *Electron transport and cytochromes in aerobically grown Proteus mirabilis*. Arch Microbiol, 1983. 136(2): p. 152-7.
[38] Baron, R., McCammon, J.A., and Mattevi, A., *The oxygen-binding vs. oxygen-consuming paradigm in biocatalysis: structural biology and biomolecular simulation*. Curr Opin Struct Biol, 2009. 19(6): p. 672-9.
[39] Orville, A.M., Lountos, G.T., Finnegan, S., Gadda, G., and Prabhakar, R., *Crystallographic, spectroscopic, and computational analysis of a flavin C4a-oxygen adduct in choline oxidase*. Biochemistry, 2009. 48(4): p. 720-8.
[40] Müller, F., and Massey, V., *Flavin-sulfite complexes and their structures*. J Biol Chem, 1969. 244(15): p. 4007-16.
[41] Massey, V., Müller, F., Feldberg, R., Schuman, M., Sullivan, P.A., Howell, L.G., Mayhew, S.G., Matthews, R.G., and Foust, G.P., *The reactivity of flavoproteins with sulfite. Possible relevance to the problem of oxygen reactivity*. J Biol Chem, 1969. 244(15): p. 3999-4006.
[42] Dym, O., and Eisenberg, D., *Sequence-structure analysis of FAD-containing proteins*. Protein Sci, 2001. 10(9): p. 1712-28.
[43] Krebs, H.A., *Metabolism of amino-acids: Deamination of amino-acids*. Biochem J, 1935 29(7): p. 1620-44.
[44] Curti, B., Ronchi, S., Branzoli, U., Ferri, G., and Williams, C.H., *Improved purification, amino acid analysis and molecular weight of homogenous D-amino acid oxidase from pig kidney*. Biochim Biophys Acta, 1973 327(2): p. 266-73.
[45] Pollegioni, L., Molla, G., Sacchi, S., Rosini, E., Verga, R., and Pilone, M.S., *Properties and applications of microbial D-amino acid oxidases: current state and perspectives*. Appl Microbiol Biotechnol, 2008. 78(1): p. 1-16.

[46] Pollegioni, L., Piubelli, L., Sacchi, S., Pilone, M.S., and Molla, G., *Physiological functions of D-amino acid oxidases: from yeast to humans*. Cell Mol Life Sci, 2007. 64(11): p. 1373-94.
[47] Pollegioni, L., Butò, S., Tischer, W., Ghisla, S., and Pilone, M.S., *Characterization of D-amino acid oxidase from Trigonopsis variabilis*. Biochem Mol Biol Int, 1993. 31(4): p. 709-17.
[48] Molla, G., Vegezzi, C., Pilone, M.S., and Pollegioni, L., *Overexpression in Escherichia coli of a recombinant chimeric Rhodotorula gracilis d-amino acid oxidase*. Protein Expr Purif, 1998. 14(2): p. 289-94.
[49] Molla, G., Sacchi, S., Bernasconi, M., Pilone, M.S., Fukui, K., and Pollegioni, L., *Characterization of human D-amino acid oxidase*. FEBS Lett, 2006. 580(9): p. 2358-64.
[50] Mizutani, H., Miyahara, I., Hirotsu, K., Nishina, Y., Shiga, K., Setoyama, C., and Miura, R., *Three-dimensional structure of porcine kidney D-amino acid oxidase at 3.0 Å resolution*. J Biochem, 1996. 120(1): p. 14-7.
[51] Kawazoe, T., Tsuge, H., Pilone, M.S., and Fukui, K., *Crystal structure of human D-amino acid oxidase: context-dependent variability of the backbone conformation of the VAAGL hydrophobic stretch located at the si-face of the flavin ring*. Protein Sci, 2006. 15(12): p. 2708-17.
[52] Duplantier, A.J., Becker, S.L., Bohanon, M.J., Borzilleri, K.A., Chrunyk, B.A., Downs, J.T., Hu, L.Y., El-Kattan, A., James, L.C., Liu, S., Lu, J., Maklad, N., Mansour, M.N., Mente, S., Piotrowski, M.A., Sakya, S.M., Sheehan, S., Steyn, S.J., Strick, C.A., Williams, V.A., and Zhang, L., *Discovery, SAR, and pharmacokinetics of a novel 3-hydroxyquinolin-2(1H)-one series of potent D-amino acid oxidase (DAAO) inhibitors*. J Med Chem, 2009. 52(11): p. 3576-85.
[53] Schell, M.J., Molliver, M.E., and Snyder, S.H., *D-serine, an endogenous synaptic modulator: localization to astrocytes and glutamate-stimulated release*. Proc Natl Acad Sci U S A, 1995. 92(9): p. 3948-52.
[54] Setoyama. C., Miura, R., Nishina, Y., Shiga, K., Mizutani, H., Miyahara, I., and Hirotsu, K., *Crystallization of expressed porcine kidney D-amino acid oxidase and preliminary X-ray crystallographic characterization*. J Biochem, 1996 119(6): p. 1114-7.
[55] Pollegioni, L., Falbo, A., and Pilone, M.S., *Specificity and kinetics of Rhodotorula gracilis D-amino acid oxidase*. Biochim Biophys Acta, 1992. 1120(1): p. 11-6.
[56] Van Veldhoven, P.P., Brees, C., and Mannaerts, G.P., *D-aspartate oxidase, a peroxisomal enzyme in liver of rat and man*. Biochim Biophys Acta, 1991. 1073(1): p. 203-8.
[57] Schräder, T., and Andreesen, J.R., *Studies on the inactivation of the flavoprotein D-amino acid oxidase from Trigonopsis variabilis*. Appl Microbiol Biotechnol, 1996. 45(4): p. 458-64.
[58] Pollegioni, L., Iametti, S., Fessas, D., Caldinelli, L., Piubelli, L., Barbiroli, A., Pilone, M.S., and Bonomi, F., *Contribution of the dimeric state to the thermal stability of the flavoprotein D-amino acid oxidase*. Protein Sci, 2003. 12(5): p. 1018-29.
[59] Zeller, A., and Maritz, A., *Uber eine neue L-aminosaure-oxydase*. Helv Chim Acta, 1944. 27: p. 1888–1903.

[60] Izidoro, L.F., Sobrinho, J.C., Mendes, M.M., Costa, T.R., Grabner, A.N., Rodrigues, V.M., da Silva, S.L., Zanchi, F.B., Zuliani, J.P., Fernandes, C.F., Calderon, L.A., Stábeli, R.G., and Soares, A.M., *Snake venom L-amino acid oxidases: trends in pharmacology and biochemistry*. Biomed Res Int, 2014. 2014: p. 196754.
[61] Duerre, J.A., and Chakrabarty, S., *l-amino acid oxidases of Proteus rettgeri*. J Bacteriol, 1975. 121(2): p. 656-63.
[62] Pelmont, J., Arlaud, G., and Rossat, A.M., *L-amino acid oxidases of Proteus mirabilis: general properties*. Biochimie, 1972 54(10): p. 1359-74.
[63] Hossain, G.S., Li, J., Shin, H.D., Du, G., Liu, L., and Chen, J., *L-Amino acid oxidases from microbial sources: types, properties, functions, and applications*. Appl Microbiol Biotechnol, 2014. 98(4): p. 1507-15.
[64] Lukasheva, E.V., Efremova, A.A., Treshchalina, E.M., Arinbasarova, A.I., Medentsev, A.G., and Berezov, T.T., *L-amino acid oxidases: properties and molecular mechanisms of action*. Biomed Khim, 2012. 58(4): p. 372-84.
[65] Yu, Z., and Qiao, H., *Advances in non-snake venom L-amino acid oxidase*. Appl Biochem Biotechnol, 2012. 167(1): p. 1-13.
[66] Vallon, O., *New sequence motifs in flavoproteins: evidence for common ancestry and tools to predict structure*. Proteins, 2000. 38(1): p. 95-114.
[67] Pawelek, P.D., Cheah, J., Coulombe, R., Macheroux, P., Ghisla, S., and Vrielink, A., *The structure of L-amino acid oxidase reveals the substrate trajectory into an enantiomerically conserved active site*. EMBO J, 2000. 19(16): p. 4204-15.
[68] Guo, C., Liu, S., Yao, Y., Zhang, Q., and Sun, M.Z., *Past decade study of snake venom L-amino acid oxidase*. Toxicon, 2012. 60(3): p. 302-11.
[69] Du, X.Y., and Clemetson, K.J., *Snake venom L-amino acid oxidases*. Toxicon, 2002. 40(6): p. 659-65.
[70] Wei, X.L., Wei, J.F., Li, T., Qiao, L.Y., Liu, Y.L., Huang, T., and He, S.H., *Purification, characterization and potent lung lesion activity of an L-amino acid oxidase from Agkistrodon blomhoffii ussurensis snake venom*. Toxicon, 2007. 50(8): p. 1126-39.
[71] Moustafa, I.M., Foster, S., Lyubimov, A.Y., and Vrielink, A., *Crystal structure of LAAO from Calloselasma rhodostoma with an L-phenylalanine substrate: insights into structure and mechanism*. J Mol Biol, 2006. 364(5): p. 991-1002.
[72] Tan, N.H., and Saifuddin, M.N., *Substrate specificity of king cobra (Ophiophagus hannah) venom L-amino acid oxidase*. Int J Biochem, 1991. 23(3): p. 323-7.
[73] Wei, J.F., Yang, H.W., Wei, X.L., Qiao, L.Y., Wang, W.Y., and He, S.H., *Purification, characterization and biological activities of the L-amino acid oxidase from Bungarus fasciatus snake venom*. Toxicon, 2009. 54(3): p. 262-71.
[74] Stiles, B.G., Sexton, F.W., and Weinstein, S.A., *Antibacterial effects of different snake venoms: purification and characterization of antibacterial proteins from Pseudechis australis (Australian king brown or mulga snake) venom*. Toxicon, 1991 29(9): p. 1129-41.
[75] Liu, J.W., Chai, M.Q., Du, X.Y., Song, J.G., and Zhou, Y.C., *Purification and characterization of L-amino acid oxidase from Agkistrodon halys pallas*

venom. Sheng Wu Hua Xue Yu Sheng Wu Wu Li Xue Bao (Shanghai), 2002. 34(3): p. 305-10.

[76] Ande, S.R., Fussi, H., Knauer, H., Murkovic, M., Ghisla, S., Fröhlich, K.U., and Macheroux, P., *Induction of apoptosis in yeast by L-amino acid oxidase from the Malayan pit viper Calloselasma rhodostoma*. Yeast, 2008. 25(5): p. 349-57.

[77] Stumpf, P.K., and Green, D.E., *l-Amino acid oxidase of Proteus vulgaris*. J Biol Chem, 1944. 153: p. 387-399.

[78] Brearley, G.M., Price, C.P., Atkinson, T., and Hammond, P.M., *Purification and partial characterization of a broad range L-amino acid oxidase from Bacillus carotarum 2Pfa isolated from soil*. Appl Microbiol Biotechnol, 1994. 41: p. 670–676.

[79] Geueke, B., and Hummel, W., *A new bacterial L-amino acid oxidase with a broad substrate specificity: purification and characterization*. Enzym Microb Technol, 2002. 31: p. 77–87.

[80] Ahn, M.Y., Ryu, K.S., Lee, Y.W., and Kim, Y.S. *Cytotoxicity and L-amino acid oxidase activity of crude insect drugs*. Arch Pharm Res, 2000. 23: p. 477–481.

[81] Palenik, B., and Morel, F.M., *Comparison of cell-surface L-amino acid oxidases from several marine phytoplankton*. Marine Ecology Progress Series, 1990. 59: p. 195–201.

[82] DeBusk, R.M., and Ogilvie, S., *Participation of an extracellular deaminase in amino acid utilization by Neurospora crassa*. J Bacteriol, 1984. 159(2): p. 583-9.

[83] Tong, H., Chen, W., Shi, W., Qi, F., and Dong, X., *SO-LAAO, a novel L-amino acid oxidase that enables Streptococcus oligofermentans to outcompete Streptococcus mutans by generating H_2O_2 from peptone*. J Bacteriol, 2008. 190(13): p. 4716-21.

[84] Faust, A., Niefind, K., Hummel, W., and Schomburg, D., *The structure of a bacterial L-amino acid oxidase from Rhodococcus opacus gives new evidence for the hydride mechanism for dehydrogenation*. J Mol Biol, 2007. 367(1): p. 234-48.

[85] Geueke, B., and Hummel, W., *Heterologous expression of Rhodococcus opacus L-amino acid oxidase in Streptomyces lividans*. Protein Expr Purif, 2003. 28(2): p. 303-9.

[86] Zhou, P., Liu, L., Tong, H., and Dong, X., *Role of operon aaoSo-mutT in antioxidant defense in Streptococcus oligofermentans*. PLoS One, 2012. 7(5): e38133.

[87] Dutra, F., Knudsen, F.S., Curi, D., and Bechara, E.J., *Aerobic oxidation of aminoacetone, a threonine catabolite: iron catalysis and coupled iron release from ferritin*. Chem Res Toxicol, 2001. 14(9): p. 1323-9.

[88] Sartori, A., Garay-Malpartida, H.M., Forni, M.F., Schumacher, R.I., Dutra, F., Sogayar, M.C., and Bechara, E.J., *Aminoacetone, a putative endogenous source of methylglyoxal, causes oxidative stress and death to insulin-producing RINm5f cells*. Chem Res Toxicol, 2008. 21(9): p. 1841-50.

[89] Baek, J.O., Seo, J.W., Kwon, O., Seong, S.I., Kim, I.H., and Kim, C.H., *Expression and characterization of a second L-amino acid deaminase*

isolated from Proteus mirabilis in Escherichia coli. J Basic Microbiol, 2011. 51(2): p. 129-35.

[90] Pantaleone, D.P., Geller, A.M. and Taylor, P.P., *Purification and characterization of an L-amino acid deaminase used to prepare unnatural amino acids*. J Mol Cat B: Enzymatic, 2001. 11: p. 795–803.

[91] Quash, G., and Fournet, G., *Methionine-derived metabolites in apoptosis: therapeutic opportunities for inhibitors of their metabolism in chemoresistant cancer cells*. Curr Med Chem, 2009. 16(28): p. 3686-700.

[92] Hossain, G.S., Li, J., Shin, H.D., Du, G., Wang, M., Liu, L., and Chen J., *One-step biosynthesis of α-keto-γ-methylthiobutyric acid from L-methionine by an Escherichia coli whole-cell biocatalyst expressing an engineered L-amino acid deaminase from Proteus vulgaris*. PLoS One, 2014. 9(12): e114291.

[93] Aparicio, M., Bellizzi, V., Chauveau, P., Cupisti, A., Ecder, T., Fouque, D., Garneata, L., Lin, S., Mitch, W.E., Teplan, V., Zakar, G., and Yu, X., *Protein-restricted diets plus keto/amino acids--a valid therapeutic approach for chronic kidney disease patients*. J Ren Nutr, 2012. 22(2 Suppl): S1-21.

[94] Song, Y., Li, J., Shin, H.D., Du, G., Liu, L., and Chen, J., *One-step biosynthesis of α-ketoisocaproate from L-leucine by an Escherichia coli whole-cell biocatalyst expressing an L-amino acid deaminase from Proteus vulgaris*. Sci Rep, 2015. 5: p. 12614.

[95] Stottmeister, U., Aurich, A., Wilde, H., Andersch, J., Schmidt, S., and Sicker, D., *White biotechnology for green chemistry: fermentative 2-oxocarboxylic acids as novel building blocks for subsequent chemical syntheses*. J Ind Microbiol Biotechnol, 2005. 32(11-12): p. 651-64.

[96] Otto, C., Yovkova, V., and Barth, G., *Overproduction and secretion of α-ketoglutaric acid by microorganisms*. Appl Microbiol Biotechnol, 2011. 92(4): p. 689-95.

[97] Hossain, G.S., Li, J., Shin, H.D., Chen, R.R., Du, G., Liu, L., and Chen, J., *Bioconversion of l-glutamic acid to α-ketoglutaric acid by an immobilized whole-cell biocatalyst expressing l-amino acid deaminase from Proteus mirabilis*. J Biotechnol, 2014. 169: p. 112-20.

[98] Okino, S., Inui, M., and Yukawa, H., *Production of organic acids by Corynebacterium glutamicum under oxygen deprivation*. Appl Microbiol Biotechnol, 2005. 68(4): p. 475-80.

[99] Hou, Y., Hossain, G.S., Li, J., Shin, H.D., Du, G., Liu, L., *Combination of phenylpyruvic acid (PPA) pathway engineering and molecular engineering of L-amino acid deaminase improves PPA production with an Escherichia coli whole-cell biocatalyst*. Appl Microbiol Biotechnol, 2015.

[100] Kato, D., Mitsuda, S., and Ohta, H., *Microbial deracemization of alpha-substituted carboxylic acids: substrate specificity and mechanistic investigation*. J Org Chem, 2003. 68(19): p. 7234-42.

[101] Breuer, M., Ditrich, K., Habicher, T., Hauer, B., Kesseler, M., Stürmer, R., and Zelinski, T., *Industrial methods for the production of optically active intermediates*. Angew Chem Int Ed Engl, 2004. 43(7): p. 788-824.

[102] Fotheringham, I., Archer, I., Carr, R., Speight, R., and Turner, N.J., *Preparative deracemization of unnatural amino acids*. Biochem Soc Trans, 2006. 34(Pt 2): p. 287-90.

[103] Turner, N.J., *Enzyme catalysed deracemisation and dynamic kinetic resolution reactions*. Curr Opin Chem Biol, 2004. 8(2): p. 114-9.
[104] Faber, K., *Non-sequential processes for the transformation of a racemate into a single stereoisomeric product: proposal for stereochemical classification*. Chemistry, 2001. 7(23): p. 5004-10.
[105] Gao, X., Ma, Q., and Zhu, H., *Distribution, industrial applications, and enzymatic synthesis of D-amino acids*. Appl Microbiol Biotechnol, 2015. 99(8): p. 3341-9.
[106] Wolosker, H., *Serine racemase and the serine shuttle between neurons and astrocytes*. Biochim Biophys Acta, 2011. 1814(11): p. 1558-66.
[107] Heller, B., *D-phenylalanine treatment*. 1982. Unites States Patent 4355044.
[108] Hertel, C., Hoffmann, T., Jakob-Roetne, R., and Norcross, R.D. *For treatment of diseases associated with amyloidosis, such as alzheimer's disease, diabetes mellitus, familial amyloid polyneuropathy, scrapie, and kreuzfeld-jacob disease*. 2000. United States Patent 6103910.
[109] Nieuwenhuijzen, J.W., Grimbergen, R.F., Koopman, C., Kellogg, R.M., Vries, T.R., Pouwer, K., van Echten, E., Kaptein, B., Hulshof, L.A., and Broxterman, Q.B., *The role of nucleation inhibition in optical resolutions with families of resolving agents*. Angew Chem Int Ed Engl, 2002. 41(22): p. 4281-6.
[110] Kim, C., and Shin, C.S., *Solvent-free enzymatic synthesis of alitame precursor using eutectic substrate mixtures*. Enzyme Microb Technol, 2001. 28(7-8): p. 611-616.
[111] Alexeeva, M., Carr, R., and Turner, N.J., *Directed evolution of enzymes: new biocatalysts for asymmetric synthesis*. Org Biomol Chem, 2003. 1(23): p. 4133-7.
[112] Isobe, K., Tamauchi, H., Fuhshuku, K., Nagasawa, S., and Asano, Y., *A Simple Enzymatic Method for Production of a Wide Variety of D-Amino Acids Using L-Amino Acid Oxidase from Rhodococcus sp. AIU Z-35-1*. Enzyme Res, 2010. 2010: p. 567210.
[113] Bifulco, D., Pollegioni, L., Tessaro, D., Servi, S., and Molla, G., *A thermostable L-aspartate oxidase: a new tool for biotechnological applications*. Appl Microbiol Biotechnol, 2013. 97(16): p. 7285-95.
[114] Enright, A., Alexandre, F.R., Roff, G., Fotheringham, I.G., Dawson, M.J., and Turner, N.J., *Stereoinversion of beta- and gamma-substituted alpha-amino acids using a chemo-enzymatic oxidation-reduction procedure*. Chem Commun (Camb), 2003. (20): p. 2636-7.
[115] Gao, X., Chen, X., Liu, W., Feng, J., Wu, Q., Hua, L., and Zhu, D., *A novel meso-Diaminopimelate dehydrogenase from Symbiobacterium thermophilum: overexpression, characterization, and potential for D-amino acid synthesis*. Appl Environ Microbiol, 2012. 78(24): p. 8595-600.
[116] Panke, S., Held, M., and Wubbolts, M., *Trends and innovations in industrial biocatalysis for the production of fine chemicals*. Curr Opin Biotechnol, 2004. 15(4): p. 272-9

[117] Wakayama, M., Yoshimune, K., and Hirose, Y., and Moriguchi, M., *Production of D-amino acids by N-acyl-D-amino acid amidohydrolase and its structure and function*. J Mol Catal B Enzym, 2003. 23: p. 71–85.
[118] May, O., Nguyen, P.T., and Arnold, F.H., *Inverting enantioselectivity by directed evolution of hydantoinase for improved production of L-methionine*. Nat Biotechnol, 2000. 18(3): p. 317-20
[119] Tessaro, D., Pollegioni, L., Piubelli, L., D'Arrigo P., and Servi S., *Systems Biocatalysis: An Artificial Metabolism for Interconversion of Functional Groups*. ACS Catalysis, 2015. 5(3): 150204115618004.
[120] Fessner, W.D., *Systems Biocatalysis: Development and engineering of cell-free "artificial metabolisms" for preparative multi-enzymatic synthesis*. N Biotechnol, 2015. 32(6): p. 658-64.
[121] Ghisla, S., and Massey, V., *New flavins for old: artificial flavins as active site probes of flavoproteins*. Biochem J, 1986. 239(1): p. 1-12.
[122] Hill, A.C., *Reversible zymohydrolysis*. J Chem Soc, 1898. 73: p. 634–658.
[123] Rona, P., et al., *Studies on the enzymatic ester formation and ester hydrolysis*. Biochem Z, 1931. 247: p. 113–145.
[124] Ashida, H., et al., *Conversion of cofactor specificities of alanine dehydrogenases by site-directed mutagenesis*. J Mol Cat B Enzym, 2004. 30: p. 173–176.
[125] Magnusson, A.O., Takwa, M., Hamberg, A., and Hult, K., *An S-selective lipase was created by rational redesign and the enantioselectivity increased with temperature*. Angew Chem Int Ed Engl, 2005. 44(29): p. 4582-5.
[126] Neuberg, C., and Hirsch, J., *Uber ein Kohlenstoffketten knupfendes ferment (Carboligase)*. Biochem. Z. (1921)115, 282–310
[127] Glasner, M.E., Fayazmanesh, N., Chiang, R.A., Sakai, A., Jacobson, M.P., Gerlt, J.A., and Babbitt, P.C., *Evolution of structure and function in the o-succinylbenzoate synthase/N-acylamino acid racemase family of the enolase superfamily*. J Mol Biol, 2006. 360(1): p. 228-50.
[128] Carlqvist, P., Svedendahl, M., Branneby, C., Hult, K., Brinck, T., and Berglund, P., *Exploring the active-site of a rationally redesigned lipase for catalysis of Michael-type additions*. Chembiochem, 2005. 6(2): p. 331-6.
[129] Da Silva, G.F., and Ming, L.J., *Catechol oxidase activity of di-Cu2+-substituted aminopeptidase from Streptomyces griseus*. J Am Chem Soc, 2005. 127(47): p. 16380-1.
[130] Yow, G.Y., et al., *Conversion of the catalytic specificity of alanine racemase to a D-amino acid aminotransferase activity by a double active-site mutation*. J Mol Catal B Enzym, 2003. 23: p. 311–319.
[131] Findrik, Z., Geueke, B., Hummel, W., and Vasic-Racki, Đ., *Modelling of l-DOPA enzymatic oxidation catalyzed by l-amino acid oxidases from Crotalus adamanteus and Rhodococcus opacus*. Biochem Eng J, 2006. 27: p. 275–286.
[132] Copley, S.D., *Toward a systems biology perspective on enzyme evolution*. J Biol Chem, 2012. 287(1): p. 3-10.
[133] Friedrich, T., and Scheide, D., *The respiratory complex I of bacteria, archaea and eukarya and its module common with membrane-bound multisubunit hydrogenases*. FEBS Lett, 2000. 479(1-2): p. 1-5.

[134] Volbeda, A., Darnault, C., Parkin, A., Sargent, F., Armstrong, F.A., and Fontecilla-Camps, J.C., *Crystal structure of the O(2)-tolerant membrane-bound hydrogenase 1 from Escherichia coli in complex with its cognate cytochrome b*. Structure, 2013. 21(1): p. 184-90.

[135] Pollegioni, L., Diederichs, K., Molla, G., Umhau, S., Welte, W., Ghisla, S., Pilone, M.S., *Yeast D-amino acid oxidase: structural basis of its catalytic properties*. J Mol Biol, 2002. 324(3): p. 535-46.

[136] Macheroux, P., Seth, O., Bollschweiler, C., Schwarz, M., Kurfürst, M., Au, L.C., and Ghisla, S., *L-amino-acid oxidase from the Malayan pit viper Calloselasma rhodostoma. Comparative sequence analysis and characterization of active and inactive forms of the enzyme*. Eur J Biochem, 2001. 268(6): p. 1679-86.

[137] Saraste, M., Sibbald, P.R., and Wittinghofer, A., *The P-loop--a common motif in ATP- and GTP-binding proteins*. Trends Biochem Sci, 1990. 15(11): p. 430-4.

[138] Lupas, A.N., Ponting, C.P., and Russell, R.B., *On the evolution of protein folds: are similar motifs in different protein folds the result of convergence, insertion, or relics of an ancient peptide world?* J Struct Biol, 2001. 134(2-3): p. 191-203.

ACKNOWLEDGMENTS

In three years the Sun releases enough energy to fuel the current worldwide needs for 47 trillion years – 3000 times the age of the universe. In the same span the earth completes three orbits around its star, covering a distance of about 3 billion kilometers, while, on average, about 400 million babies are born. In three years each tree produces up to 900 kg of oxygen to keep them alive.

Wondrous things can be accomplished in such a short period of time. Even a man, with his 110 million heartbeats, in his own small way can achieve something important. But all of this wouldn't be possible without the help of many other "teammates".

First of all I would like to thank prof. Loredano Pollegioni for the opportunity to work in his laboratory.
I thank prof. Gianluca Molla for his supervision during this period: without his guiding light I would have ineluctably drifted through the sea of my ignorance.

Most importantly, Alessia: even if in the end things didn't go the way we expected, I owe much of this PhD to you. Thank you for everything.

I would like to thank Laura, Pamela and Paola, for the patience with which they have endured this nuisance of a man. Without you everything would have been harder.

A special thanks goes to Jessica and Valentina for the invaluable effort they put in their work. A good half of this thesis was possible because of you.

Thanks to the “neverending” Gianluchino, Giulia and Zoraide for all the laughs in these years.

A big thank you to all the other people in the lab, be them researchers, post-doc or students, past or present, which are too many to be mentioned one by one, hence I will: Luciano, Silvia, Elena, Luca, Gianluca (yes, another one), Davide, Fabio, Roberta, Patrick, Valentina, Alberto, Tommaso, Alessandro, Andrea, Jennifer, Simona, Andrea, Alice, Alessandra and Lorenza. I hope the ones I forgot will forgive me.

They have been three beautiful years. Thank you all.